
Heinrich summers

Denton George H. ¹, Toucanne Samuel ², Putnam Aaron E. ^{1,*}, Barrell David J.A. ³, Russell Joellen L. ⁴

¹ School of Earth and Climate Science and Climate Change Institute, University of Maine, Orono, ME 04469, USA

² Univ Brest, CNRS, Ifremer, Geo-Ocean, F-29280, Plouzane, France

³ GNS Science, Dunedin, New Zealand

⁴ Department of Geosciences, University of Arizona, AZ, USA

* Corresponding author : Aaron E. Putnam, email address : aaron.putnam@maine.edu

Abstract :

Millennial-scale climate oscillations of the last ice age registered in Greenland and Antarctic ice cores did not always vary in unison. A striking example is that the strongest Antarctic warming episodes occurred during Heinrich episodes in the North Atlantic region. Although the bipolar seesaw affords a possible explanation for such anti-phasing, it does not account for the equally striking observation that climate varied in unison between the hemispheres about half the time. Such phasing differences suggest the need for an alternative hypothesis in which the polar regions at times responded in unison to common forcing, and at other times left the impression of a bipolar seesaw. We posit that this impression arose from the effect of warmer-than-usual summers on continental ice sheets adjacent to the North Atlantic Ocean during each Heinrich episode. The relatively warm Heinrich summers produced discharges of meltwater and icebergs of sufficient volume to stimulate very cold winter conditions from widespread sea ice on a freshened ocean surface. The intervals between Heinrich episodes featured relaxation of sea-ice-induced winter severity from reduced summertime influx of meltwater and icebergs, indicating relatively cooler summer conditions. It is postulated that the causative variations in freshwater fluxes were driven by a climate signal most evident in Antarctic ice cores but also recognized in other paleoclimate records in both polar hemispheres. We suggest that this widespread signal arose from changes in the latitude and strength of the austral westerlies and the resulting effect on the western Pacific tropical warm pool, a mechanism dubbed the Zealandia Switch.

Highlights

► Bipolar synchrony of millennial-scale glacier melt during the last glaciation. ► Interhemispheric glacier signal inconsistent with 'bipolar seesaw' hypothesis. ► Northern 'stadials' attributed to warm summers paired with extremely cold winters. ► Enhanced melt-induced northern seasonality obscured global ice-age climatic signature. ► Differentiating summer from winter effects key to interpreting paleoclimatic proxies.

Keywords : Climate dynamics, Glacial, Glaciation, Seasonality, Heinrich stadials, Termination, Pleistocene, Paleoclimatology, Antarctica, Greenland, North Atlantic, North America, Western Europe, Cosmogenic isotopes, Geomorphology, Ice cores, Sedimentology-marine cores

41 **Introduction**

42

43 The origin of recurring millennial-scale climate oscillations in both polar hemispheres during the
44 last ice age and its termination remains elusive. Figure 1 illustrates these oscillations as they
45 appear in the isotopic signatures of Greenland and Antarctic ice cores. A determination of why
46 changes represented in these records did not always vary together lies at the heart of
47 understanding the relationship of ice-age climate oscillations between the hemispheres. It has
48 long been noted that the warming phases of Antarctic Isotopic Maxima (AIM) coincided with
49 Greenland Heinrich stadials (HS) (e.g., Pedro et al., 2018 and references therein). However, less
50 commonly highlighted is the observation (Steig and Alley, 2002) that Antarctic and Greenland
51 climate oscillations during the last glacial cycle showed such anti-phased behavior only about
52 50% of the time, interspersed with in-phase changes, particularly during cooling ramps that
53 followed warm peaks (Figure 1). Moreover, there is an important structural difference between
54 the ice-core isotopic signatures of the two polar hemispheres in that the Greenland oscillations
55 featured fast climate shifts, unlike the Antarctic oscillations.

56

57 Any hypothesis for the origin of climate oscillations as registered in ice-core records should
58 account for the structural difference, as well as for the temporal relationships, between
59 Greenland and Antarctic oscillations. A prominent hypothesis for the temporal linkage features a
60 “bipolar seesaw” in which cooling in one polar hemisphere was countered by warming in the
61 other polar hemisphere, and vice versa. We investigate the origins of ice-age millennial-scale
62 climate variations through the comparison of mid-latitude glacier-derived records, one from the
63 Northern Hemisphere comprising meltwater-sourced sediment deposited offshore from the
64 mouth of the ice-age Channel River between France and England, the other from Southern
65 Hemisphere glacial moraines in the Southern Alps of New Zealand. Together with other proxy
66 records, we re-evaluate whether the bipolar seesaw still offers an adequate explanation of
67 millennial-scale climate shifts, or whether there are better alternatives.

68

69

70 **Channel River discharge record**

71

72 During the maximal phase of the last glaciation [i.e., Last Glacial Maximum – LGM; 26.5-19 ka
73 (Clark and Mix, 2002; Clark et al., 2009)], when the sea was at or near its lowest level, the
74 coalescence of the Scandinavian and British-Irish ice sheets (northwest European ice sheets -
75 EIS) over the area of the present-day North Sea caused rearrangement of western Europe fluvial
76 drainage. Runoff from the southern parts of the EIS merged with drainage from the northwestern
77 part of the Alps to create the west-flowing Channel River, which discharged into the Bay of
78 Biscay (Figure 2). With a catchment area similar to that of North America’s Mississippi River,

79 the Channel River was a dominant contributor of fresh water input to the eastern North Atlantic
80 Ocean (Gibbard, 1988; Zaragosi et al., 2001; Ménot et al., 2006; Toucanne et al., 2009, 2010;
81 Boswell et al., 2019).

82 The records of Channel River discharge come from well-dated marine sediment cores from near
83 the former river mouth (Zaragosi et al., 2001; Ménot et al., 2006; Eynaud et al., 2007, 2012;
84 Toucanne et al., 2009, 2015). Particularly important is core MD95-2002 (Figure 2), whose
85 neodymium isotope composition of the fine-sediment fraction links the detrital sediment in the
86 core with a source along the southern sector of the EIS (Toucanne et al., 2015). Paleo-discharge
87 variations are interpreted from the reconstruction of regional sediment flux and ratios of major
88 elements based on XRF data measured in core MD95-2002, and in other nearby cores (Toucanne
89 et al., 2015). The ratios of Ti/Ca and Fe/Ca register terrigenous inputs and, by extension, past
90 discharge from the Channel River, with higher versus lower values respectively indicating
91 increased or decreased discharge (Figure 3). The links between ice-marginal fluctuations and
92 discharge of the Channel River come from a comparison of the core parameters with moraine
93 chronologies in the source areas (Toucanne et al., 2015). In particular, increased meltwater flow
94 near the end of the last glaciation coincided with ice-margin retreat. Toucanne et al. (2015)
95 concluded that the varying flow of the Channel River monitored the melt response of the EIS to
96 changing summer temperature. Intervals of notably greater runoff are taken to reflect warmer
97 summer temperatures and are labeled, from older to younger, R1-R5. R1 corresponds in time
98 with HS3, R2 with HS2, and R5 with the first half of HS1. R3 and R4 represent increased runoff
99 episodes not recognized as Heinrich stadials. That the Heinrich stadials are interpreted as cold
100 intervals highlights a conundrum: why did increased meltwater discharge from the Channel
101 River occur during cold climate episodes? This problem is underscored by a similar finding that

102 the Danube River, which drained melt from ice-age glaciers of the northeastern Alps, also had
103 increased discharge during Heinrich stadials (Martinez-Lamas et al., 2019).

104

105

106 **Southern Alps moraine record**

107

108 A detailed chronology of alpine glacier fluctuations adjacent to the highest parts of New
109 Zealand's Southern Alps is based on exposure-ages of boulders concentrated in moraine belts
110 (Figure 4) or as erratics on glacially-shaped landscapes (Schaefer et al., 2006, 2009, 2015;
111 Kaplan et al., 2010, 2013; Putnam et al., 2010a, 2010b, 2012, 2013a, 2013b; Barrell et al., 2011;
112 Kelley et al., 2014; Doughty et al., 2015; Koffman et al., 2017; Strand et al., 2019; Denton et al.,
113 2021). In the mid-latitude maritime climatic setting of the Southern Alps, summer melt
114 determined by austral summer season temperature is the major driver of the annual snowline
115 (ELA) position and hence for fluctuations of the glaciers that produced the moraine belts
116 (Anderson, 2005; Anderson et al., 2006; Anderson and Mackintosh, 2006; Anderson et al., 2010;
117 Anderson and Mackintosh, 2012; Lorrey et al., 2014; Purdie et al., 2014; Koffman et al., 2017;
118 Mackintosh et al., 2017; Lorrey et al., 2022). Modeling of glacier extent targeting dated moraine
119 belts, and employing precipitation values ranging 0-30% less than modern, indicates that
120 temperatures necessary for glaciers to occupy moraine belts of full-glacial extent were 6-7°C
121 cooler than modern. The late-glacial moraines farther up the catchments relate to temperatures 2-
122 3°C cooler than present.

123 Construction of the moraine belts marked the culminations of glacier expansion, followed by

124 glacier retraction that resulted in the moraine belt being preserved. The overall pattern of glacier

125 fluctuations follows a Heinrich pulsebeat in which moraine construction occurred in intervals
126 between Heinrich stadials, with no moraines preserved from the stadials themselves (Figure 3).
127 This pattern of southern moraine construction between northern stadials (Strand et al. 2019)
128 characterized not only the last glaciation but also the last termination. Rapid, large-scale, glacier
129 retreat began at ~18 ka, with the demise of ice-age glaciers during HS1 (17.8 to 14.7 ka)
130 equating to 75% of the glacial/interglacial climate transition in the Southern Alps, with near-
131 interglacial conditions attained by the end of HS1 (Denton et al. 2021). This sustained glacier
132 retraction was followed by glacier resurgence during the Antarctic Cold Reversal (ACR, coeval
133 with the northern Bølling-Allerød interstadial) and then further retreat during HS0 (approximates
134 Younger Dryas from 12.9 to 11.7 ka). Comparison with the isotope signature from the South
135 Pole ice core (Figure 5) highlights a prominent southern registration of the Heinrich stadials
136 (interpreted as warming conditions). Southern Alps moraines formed during intervening times,
137 where the isotope signature indicates cooler conditions.

138

139

140 **Significance of the Channel River and Southern Alps records**

141

142 The two records show close alignment of reduced discharge from the Channel River (troughs in
143 the Ti-Fe curve) and alpine glacier moraine formation in the Southern Alps (Figure 3). Insofar as
144 the Channel River discharge comprised substantial meltwater from the EIS, minima of discharge
145 imply minima of melt, attributable to cooler climate conditions with net ice accumulation.
146 Southern Alps glacier expansion similarly implies cooler temperatures. Greater Channel River
147 discharge during Heinrich stadials, and coeval absence of Southern Alps moraine formation in

148 the full-glacial moraine belts, suggest warmer temperatures in both regions. Rather than showing
149 a bipolar seesaw pattern, notable synchronicity is evident between the Channel River and the
150 Southern Alps records.

151

152

153 **Concept framework**

154

155 The bipolar seesaw is a hypothesis for millennial-scale differences between Greenland and
156 Antarctic isotopic signatures in ice cores. A favored mechanism is interhemispheric
157 redistribution of heat through an oceanic seesaw, augmented by atmospheric components (e.g.,
158 Pedro et al., 2011, 2018; WAIS Divide Project Members, 2015). A deep-water version of the
159 seesaw posits that the interhemispheric temporal linkage arose from alternations in ocean heat
160 transport caused by perturbations in the relative strengths of formation of North Atlantic Deep
161 Water and Antarctic Bottom Water (Broecker, 1998). Another version of the seesaw is based on
162 the effects of variations of Atlantic overturning circulation on the transport of near-surface ocean
163 heat across the equator (Crowley, 1992; Stocker and Johnsen, 2003).

164

165 Assuming that the ocean/atmosphere bipolar seesaw hypothesis is correct, then a small temporal
166 lead of Greenland climate breakpoints over their Antarctic counterparts has been interpreted as
167 indicating a Northern Hemisphere origin for millennial-scale temperature shifts, with the North
168 Atlantic region being the likely source (WAIS Project Members, 2015). The possibility is
169 acknowledged that the Greenland breakpoints may have been a response to a “remote process not
170 visible in the ice core records” (WAIS Project Members, 2015).

171

172 In contrast, the Channel River and Southern Alps records, as one comparative example of mid-
173 latitude data, show a view of interhemispheric synchrony (within age uncertainties) of shifts to or
174 from episodes of generally warmer summers. Examining data from the middle latitudes, where
175 seasonality is prominent, we explore the idea that the millennial-scale stadials of the last
176 glaciation and termination were inter-regional expressions of globally uniform climate
177 oscillations.

178

179

180 **Northern Hemisphere oceanic signatures**

181

182 Heinrich stadial episodes encompassed distinctive signatures in Greenland ice core $\delta^{18}\text{O}$ and in
183 peaks of North American ice-rafted debris (IRD) deposition, called Heinrich events. Increased
184 IRD deposition was a feature of Heinrich stadials not just generally in the northern North Atlantic
185 but also more specifically in proximity to major ice streams of the Northern Hemisphere ice sheets,
186 including the North Pacific (Walczak et al., 2020; Figure 6a-c). These recurring episodes of ice
187 discharge from Northern Hemisphere ice sheets into two oceans implies widespread rather than
188 localized ice-sheet instability. In unison with increased sediment deposition during HS3, HS2 and
189 HS1 (Figure 6c-d), relatively warmer conditions in summer offers, in our view, a likely explanation
190 for these observations. Thus, we suggest that the progressive warming registered in isotopic
191 records from Antarctic ice during Heinrich stadials (Figure 6e) is indicative of a widespread
192 phenomenon, as exemplified in the comparison of the Channel River and Southern Alps records
193 (Figure 3).

194

195 Sedimentary archives from the North Atlantic region yield elements of two millennial-scale
196 climate signals, one similar to that in the atmosphere over Greenland and the other similar to that
197 in the atmosphere over Antarctica as registered in ice cores. According to Rasmussen et al.
198 (2016), the Greenland signal equates to stratification of the water column through formation of a
199 surface layer of cold, low-salinity water, linked to an influx of meltwater and/or icebergs. The
200 Greenland signal is prominent in records from the Nordic Seas (Rasmussen and Thomsen 2008),
201 in the Ruddiman ice-rafting belt (Rasmussen et al., 2016), near the Bermuda Rise (Gil et al.,
202 2009; Henry et al., 2016), in the eastern North Atlantic near the Iberian Peninsula (Sánchez Goñi
203 et al., 2000; Shackleton et al., 2000), as well as in the western Mediterranean basin (Sánchez
204 Goñi et al., 2002). In contrast, the Antarctic signal is evident in open marine areas which
205 experienced only modest influxes of Heinrich stadial icebergs (Rasmussen et al. 2016), such as
206 near the Reykjanes Ridge (Rasmussen et al., 2016) and in the southern and central North Atlantic
207 (Ruhlemann et al., 1999; Pahnke and Zahn, 2005; Peck et al., 2008; Naafs et al., 2013;
208 Guilderson et al., 2021), with an example illustrated in Figure 7. A common explanation for cold
209 conditions during Heinrich stadials is that a low salinity surface layer of the North Atlantic
210 Ocean afforded a platform for the widespread formation of sea ice (Denton et al., 2005).

211

212

213 **Seasonality in the North Atlantic and western Europe regions**

214

215 Contrasts in seasonality are suggested to have played a central role in the signatures of
216 Greenland ice-core and moraine records from the last glaciation and termination (Denton et al.,

217 2005). From thermally fractionated gases in the GISP2 ice core, the Younger Dryas/HS0 section
218 shows a mean annual temperature 15°C colder than today at the Greenland summit
219 (Severinghaus et al.,1998). In contrast, the positions of late-glacial moraines of outlet glaciers in
220 the coastal mountains near Scoresby Sound in southeastern Greenland (Figure 8) indicate
221 Younger Dryas summertime temperature no more than a few degrees cooler than today. In
222 combination with the ice-core registered mean annual temperature, these relatively mild summer
223 temperatures imply an average winter temperature 26-28°C cooler than today (Denton et al.,
224 2005; Broecker, 2006). Such marked seasonality is best explained by an extensive Younger
225 Dryas winter sea ice cover on the North Atlantic Ocean (Denton et al., 2005; Broecker, 2006).

226

227 A more recent chronologic study of moraines related to late-glacial ice recession in southeastern
228 Greenland in the Scoresby Sound region suggests that summers may have become progressively
229 warmer during the Younger Dryas (Levy et al., 2016). If so, seasonality would have been even
230 greater than shown in Figure 8. In accord with these new chronological data from Scoresby
231 Sound, Funder et al. (2021) and Carlson et al. (2021) documented ice retreat along Greenland's
232 southwestern coast and noted recession from elsewhere along the ice-sheet margin during
233 Younger Dryas time. These results from Greenland are further supported by evidence from the
234 Scottish Highlands (Bromley et al., 2014; 2018) and from northern Norway (Wittmeier et al.,
235 2020) for glacial recession during Younger Dryas time.

236 The overall result reflects Younger Dryas seasonality, with ice-sheet margin recession
237 due to the effect of warm summers on the peripheral ablation zone, paired with exceptionally
238 cold winters that collectively produced an overall very cold mean annual temperature registered,

239 for example, in the GISP2 ice core from the summit of the Greenland Ice Sheet (Severinghaus et
240 al., 1998).

241

242 Extreme seasonality is also indicated for late glacial time in northwestern Europe from subfossil
243 remains of species of plants and beetles, together with evidence for the distributions of
244 permafrost. The results show extremely cold winter temperature and no more than modestly
245 cooler summers during HS1 and the Younger Dryas, thus providing further evidence of late-
246 glacial episodes of winter-dominant extreme seasonality. A shift to substantially less cold
247 winters heralded a return to normal seasonality with warmer mean annual temperatures that
248 characterized the Bølling and the Holocene (Atkinson et al., 1987; Isarin, 1997; Isarin et al.,
249 1998; Isarin and Bohncke, 1999; Renssen and Isarin, 2001; Renssen and Bogaart, 2003). The
250 central role of North Atlantic sea ice in producing the winter-dominant cold pulses evident both
251 in the Greenland ice-core and in the northwest European terrestrial records has been widely
252 discussed in the literature. There is much support for the late glacial climate record of millennial
253 change of northwestern Europe reflecting variations of the sea-ice cover on the North Atlantic
254 Ocean (e.g., Li et al., 2005; Fluckiger et al., 2008; Sime et al., 2019).

255

256 Other biological records also highlight an association of millennial-scale climatic shifts and
257 varying seasonality. For example, in marine sediment core MD95-2042 collected near the
258 southwestern margin of the Iberian Peninsula, the oxygen-isotope signature from planktonic
259 foraminifera mimics the Greenland isotopic pattern, whereas the benthic foraminifera oxygen
260 isotope record is similar to Antarctic ice-core isotopic signals (Shackleton et al., 2000).

261 Seasonality is also expressed in paleo-vegetation records from pollen spectra, which follow the

262 Greenland signal, not the Antarctic signal (Sánchez Goñi et al., 2000). Winter cold and dry
263 intervals on the Iberian Peninsula accompanied the Heinrich and Dansgaard/Oeschger cold
264 stadials registered in Greenland ice. Another example is provided by marine sediment core
265 MD95-2043 from the western Mediterranean Sea (Sánchez Goñi et al., 2002), where the sea-
266 surface temperature (SST) indicators and pollen signatures in MIS 3 co-vary together with a
267 Greenland pattern. The pollen shows alternating steppe (stadial) and Mediterranean forest
268 (interstadial) biomes, while the mean SST implies cold stadial winters (as does the SST record
269 from MD95-2042).

270

271 If there is merit in the view that the climate variability interpreted from Greenland ice cores is
272 heavily weighted toward the winter season (Denton et al. 2005; Broecker, 2006; Buizert et al.,
273 2014, 2018; He et al., 2021), then the parallelism between ice-core and vegetation records
274 suggests that the millennial variability of southern European vegetation resulted largely from
275 wintertime forcing, with Greenland temperature and European vegetation distribution both
276 following North Atlantic winter sea ice. We think that winter conditions severe enough to
277 preclude some species of trees and other frost-sensitive vegetation from the European landscape
278 would likely hamper attempts to interpret summer temperatures from vegetation records. This is
279 apparent, for example, in paleoclimate records from Switzerland. Lake marl at Gerzensee on the
280 northern border of the Alps yielded high-resolution stacked isotopic records showing the
281 distinctive switch from Oldest Dryas (HS1) to Bølling climate, as well as the patterns of the
282 Younger Dryas and minor oscillations such as the Gerzensee and Aegelsee cool climate episodes
283 (Siegenthaler et al., 1984; Van Raden et al., 2013). The Gerzensee pollen record has the Oldest
284 Dryas section dominated by open herb-shrub tundra vegetation, bereft of birch and pine trees,

285 followed by the iconic juniper peak at the boundary between the Oldest Dryas and the Bølling,
286 approximately coeval with the isotopic switch (Ammann et al., 2013). A hallmark of the Bølling
287 was the first appearance of late-glacial trees, with birch first, followed by pine, and within a few
288 centuries the landscape supported birch/pine woodland. Permafrost was probably present near
289 Gerzensee in Oldest Dryas time, but had melted out by early in the Bølling (Ammann et al.,
290 2013). Other sites revealing characteristic Oldest Dryas steppe-tundra vegetation occur on the
291 Swiss plateau, as well as in formerly glaciated valleys well inboard of the LGM ice limits
292 (Eicher and Sigenthaler, 1976; Burga, 1988). From these data, Burga (1988) concluded that
293 *Artemisia* steppe-tundra dominated the Oldest Dryas vegetation prior to the onset of the Bølling,
294 and that such sites inside the LGM ice limit demonstrate that immediately following the LGM,
295 glaciers receded deep into the Alps, leaving only the high passes still glaciated. This was
296 considered to reflect summer melting. During subsequent Bølling time, the vegetation records
297 showed the spread of birch, pine, and juniper on a landscape already deglaciated. Thus, strong
298 seasonality associated with HS1 is registered in the Swiss records.

299

300

301 **Heinrich Summers hypothesis**

302

303 Available data present two major difficulties for the bipolar seesaw concept. First is the
304 observation of Steig and Alley (2002) that the Antarctic and Greenland ice-core proxy climate
305 records are anti-phased for only about 50% of the time, but show closely similar signatures of
306 change during the remaining 50%. Second, the characterization of Greenland stadials as
307 fundamentally cold climate episodes is at odds with the concept of extreme seasonality, featuring

308 hyper-cold winters but generally mild summers. A seesaw model thus offers at best only a partial
309 explanation for the ice-core isotopic patterns. But it is not in accord with the comparison of
310 summer-dominated ice melt records from northern Europe with glacier advance/retreat at an
311 equivalent latitude in the Southern Hemisphere (Figure 3). Both records indicate glacier melt in
312 their respective summer seasons. They show that the anti-phasing between the hemispheres seen
313 in ice-core records disappears when specifically considering summer conditions. Here we
314 propose an alternative explanation for the apparently anti-phased parts of the record, dubbed the
315 Heinrich Summers hypothesis, focused on the climatic effects of abundant summer meltwater in
316 the North Atlantic Ocean. Attention is directed here towards the Heinrich oscillations, which
317 appear to have had stronger climatic imprints than the Dansgaard/Oeschger oscillations, although
318 similar general principles apply to both.

319

320 A natural conditioning toward seasonality in northern latitudes exists because the two polar
321 hemispheres have contrasting geographical configurations, with the northern featuring huge
322 continents and the southern being ocean-dominated. In the Heinrich Summers hypothesis, the
323 structural and temporal differences in ice-age millennial-scale climate signals between the two
324 polar regions arises from differing amplifications of seasonality. The amplification of northern
325 seasonality was strongly linked to the presence of substantial ice-age ice sheets on northern
326 North America and northern Europe. Freshwater delivery into the North Atlantic Ocean, through
327 both influent meltwater and melting icebergs, presents a mechanism for the formation of a low
328 salinity surface water stratum in the ocean, which is then susceptible to extensive winter
329 freezing. During the last ice age whenever the northern North Atlantic was covered with sea ice,
330 a huge sector of the Northern Hemisphere stretching from North America to eastern Asia became

331 essentially continental, leading to extreme seasonality marked by exceptionally cold winters
332 (Denton et al., 2005). This raises the question of what caused the northern climate to cross this
333 threshold into extreme seasonality. A counterintuitive answer is that the change resulted from a
334 shift to warmer summers that stimulated increased ice melt and iceberg discharge into the North
335 Atlantic Ocean from European and North American ice sheets, leading to exceptional winter sea
336 ice on the summer-freshened ocean surface. By this view, the northern ice-age stadial signature
337 is an expression of extreme seasonality (Denton et al., 2021).

338

339 The correspondence in the timing of Northern Hemisphere Heinrich episodes, related to
340 enhanced iceberg-and-meltwater discharges, and Southern Hemisphere mountain glacier
341 recession, points to the occurrence of episodes of warmer summers in both hemispheres. By the
342 Heinrich Summers hypothesis, the Cordilleran, Laurentide, Greenland, Barents, Scandinavian,
343 and British/Irish ice sheets responded to each Heinrich warming episode by net ice loss, with two
344 examples of warmer conditions being the Channel River meltwater outflow and Hudson Strait
345 ice discharge (Toucanne et al., 2015; Zhou et al., 2021). A likely consequence of the resulting
346 extensively freshened sectors of the surface of the North Atlantic Ocean (Rasmussen et al., 2016)
347 would have been a weakening of the Atlantic Meridional Overturning Circulation (AMOC)
348 (Bohm et al., 2015; Henry et al., 2016), providing a further feedback that stimulated expansion of
349 winter sea ice. The sea-ice lid would also have reduced heat exchange between the ocean and the
350 atmosphere. As a result, the winter climate of the North Atlantic region during each Heinrich
351 episode would have switched from maritime to continental, with greatly increased summer-
352 winter seasonality over the course of each year. In sum, warm summers generated glacier melt,
353 which then produced a derivative signal of very cold winters via the consequent rollout of sea ice

354 and reduction of the AMOC. Because the effects were so strong in the North Atlantic region, the
355 large winter sea-ice signal overpowered any smaller summer signature in Greenland ice cores,
356 with the possible exception of the HS1 episode (He et al., 2021). Modelling experiments
357 highlight a linear relationship between the extent of North Atlantic winter sea ice and the air
358 temperature over central Greenland (Roberts and Hopcroft, 2020). By the Heinrich Summers
359 hypothesis, the excessively cold northern stadial winters closely linked to summer melt of
360 adjacent ice sheets create a false impression of a bipolar seesaw with Southern Hemisphere
361 climate.

362

363 Stratification of the northern North Atlantic Ocean surface water under ice-age stadial conditions
364 is suggested to have inhibited heat loss from subsurface water (Rasmussen et al., 2016; Su et al.,
365 2016). This may have led to subsurface ocean warming that could have enhanced subsurface
366 melting at ice-sheet grounding lines (Shaffer et al., 2004; Marcott et al., 2011). Recent analogs
367 are afforded from West Greenland (Holland et al., 2008) and West Antarctica (Joughin et al.,
368 2021), where melt-driven thinning at grounding lines is suggested to have resulted in speedup of
369 ice streams. This mechanism may also account for the greatly enhanced iceberg production that
370 characterized Heinrich episodes (Shaffer et al., 2004; Marcott et al., 2011). Of particular note is
371 the finding that the increase in IRD routinely followed the onset of Heinrich climate conditions
372 (Barker et al., 2015), suggesting that iceberg generation was a consequence, not a cause, of those
373 conditions.

374

375 Superimposition of the Greenlandic and Antarctic isotopic records (Figure 1) highlights the
376 strong similarity of the records, apart from the differences during Greenland stadial episodes. By

377 the Heinrich Summers hypothesis, the Antarctic AIM episodes, which are paired with the
378 Greenland stadials (both Heinrich and Dansgaard/Oeschger), are an expression of a foundational
379 global signal of millennial-scale climate oscillations, in alignment with the proposition of Barker
380 and Knorr (2007) that the Antarctic ice-age climate signal was globally pervasive. The Antarctic
381 signature being an expression of climate shifts of global reach is consistent with the
382 interpretation of summer warmth in melt records of the Channel River during HS1, HS2, and
383 HS3. Moreover, there are indications of warm Younger Dryas (HS0) summers in Europe
384 (Schenk et al., 2018), in step with the Younger Dryas ice-marginal retreat described above for
385 Greenland. During such North Atlantic extreme-seasonality episodes, we suggest that the
386 Greenland winter signal so dominated the mean annual temperature there that a global signature
387 of relatively warm summers was masked. Nevertheless, western Europe records that are directly
388 linked to summer conditions, such as the Channel River meltwater discharge, illustrate the
389 occurrence of relatively warm summers accompanying North Atlantic winter stadials. The notion
390 of warm summers associated with winter stadials is also exemplified by the large-scale retreat
391 exhibited during HS1 by ice-age glaciers to positions deep within the European Alps, as shown
392 by the occurrence of Oldest Dryas pollen signatures in post-glacial sediments.

393

394 Terrestrial records, such as pollen, might at first glance be interpreted as showing cold summers
395 during Heinrich episodes, such as illustrated by the iconic representation of the tundra plant
396 *Dryas octopetala*. However, an alternative possibility is that only frost-tolerant vegetation
397 survived the severely cold stadial winters. The imprint of North Atlantic winter stadial conditions
398 is highlighted by the extensive persistence of tundra vegetation and permafrost in mid-latitude
399 Europe during the Oldest Dryas (Renssen and Isarin, 2001). The replacement of tundra by

400 temperate vegetation, including forest, proceeded rapidly at the onset of the Bølling interstadial.
401 The findings of Renssen and Isarin (2001) of a recovery of at least 15°C in winter (January)
402 temperature across the Oldest Dryas/Bølling boundary can be interpreted as a return to normal
403 seasonality, in the Heinrich Summers hypothesis. This importance of winter-limiting controls on
404 vegetation is illustrated, for example, by the modern United States Department of Agriculture
405 plant hardiness zone map of North America (Daly et al., 2012), which uses winter coldest
406 temperatures as a major determinant of which species can survive in which winter climate zone.
407 We suggest that warmth of summer climate is difficult to determine from vegetation records if
408 the winter climate is too cold to allow survival of key elements of the vegetation in the first
409 place. The example of the mismatch in the Swiss evidence from Oldest Dryas time, where
410 glaciers receded far back into the Alps, but trees had yet to appear on the alpine foreland that
411 remained characterized by the herbs and shrubs of Oldest Dryas tundra, is an example of a high
412 degree of seasonality associated with winter stadial conditions in the North Atlantic region.
413
414 We postulate that North Atlantic seasonality was normal when the Greenland and Antarctic ice-
415 core isotopic signals (Figure 1) varied in approximate unison, but the two patterns diverged when
416 North Atlantic seasonality was exceptionally strong. The classic stadial/interstadial oscillations
417 registered in Greenland ice cores are illustrated in relation to HS4 and HS5 in Figure 1c-d.
418 Following an initial pronounced warming peak representing a Greenland interstadial, there
419 ensued a parallel cooling ramp in both signals for the remainder of the interstadial. An
420 approximately coeval change saw the onset of a rising (warming) trend in the Antarctic signal,
421 while the Greenland signal dropped to prolonged minimal values marking the low mean annual
422 temperatures associated with North Atlantic extreme seasonality, dominated by exceptionally

423 cold winters. A key relationship is expressed when each Greenland stadial ended. The Greenland
424 isotope signature abruptly rebounded to align closely with the Antarctic signature. By the
425 Heinrich Summers hypothesis, we attribute the stadial signal to extreme northern winters,
426 without which we suggest the Greenland and Antarctic signals would be broadly the same. In
427 that regard, we propose that the trend of warming seen in Antarctica during northern winter-
428 dominated climatic episodes illustrates in general terms what the character of northern summers
429 may have been like during episodes of winter-stadial climate. We consider that the Greenland
430 peak interstadials reveal the true nature of summer climate there, when unmasked from the
431 overpowering signature of extremely cold winters.

432

433 We suggest that the Antarctic isotopic signature is a regional expression of climatic shifts arising
434 elsewhere, for example in the mid-latitudes and tropics as described by the Zealandia Switch
435 hypothesis (Denton et al., 2021). We take the subdued nature of the rising and falling ice-core
436 isotopic trend of each AIM event to indicate that the Southern Ocean was slow to heat following
437 a shift to warmer climate, and that the Antarctic signature is primarily associated with high-
438 latitude Southern Ocean conditions. We view the abrupt onset of each millennial-scale climatic
439 ‘stadial’ in the Greenland record as indicating a rapid shift to warmer summers that generated a
440 prominent increase in meltwater discharge into the North Atlantic Ocean. Similarly, we envision
441 the abrupt end to each ‘stadial’ as reflecting a shift in climate of global reach to cooler summer
442 conditions that notably lessened meltwater input such that the cold and low-salinity surface layer
443 on the North Atlantic could not be maintained. The resulting weakening of the cap of cold, low-
444 salinity water and sea ice allowed relatively warm and saline subsurface water, which had built
445 up at depth during the stadial, to punch through the surface stratification and release heat into the

446 atmosphere (for discussion of various aspects of subsurface warming and/or overturning of the
447 stratified water column see, for example, Shaffer et al., 2004; Marcott et al., 2011; Rasmussen
448 and Thomsen, 2004; Thiagarajan et al., 2014; Guilderson et al., 2021). This caused an abrupt end
449 to extreme seasonality, with the greatest change in winter. A repeated return of a normal
450 seasonality condition through this mechanism could have produced the repeated iconic warm
451 jumps seen in Greenland isotopic signatures. To explain the classic signature of the
452 Dansgaard/Oeschger events, interpreted as comprising an abrupt warming succeeded quickly by
453 a strong cooling trend, we posit that a shift to cooler summers reduced the meltwater flux and in
454 turn winter sea ice extent, thus releasing the North Atlantic regional climate back to normal
455 seasonality.

456

457

458 **Discussion**

459

460 The Heinrich Summers hypothesis has two major tenets. One is that the ice-age millennial-scale
461 climate oscillations arose from temperature variations of global scope. By this hypothesis, the so-
462 called Antarctic climate signal is regarded as a general representation of the character of the
463 millennial-scale oscillations in both hemispheres. The second major tenet is that the anti-phased
464 relations within the millennial-scale climate oscillations registered in Antarctic and Greenland
465 ice cores is due to an exceptional rollout of sea ice in the North Atlantic that was a derivative
466 winter response to global warming during each oscillation episode. This derivative winter
467 response dominated Greenland isotopic signatures, giving the impression, when viewed in
468 isolation, of a bipolar seesaw of climate change between the two polar hemispheres.

469

470 There are several lines of evidence, in addition to those described above, that reinforce the view
471 that the Antarctic signal reflects global climate shifts. One is the meltwater signal produced by
472 variations in the flow of the Mississippi River, when it drained the southern sector of the
473 Laurentide Ice Sheet to the Gulf of Mexico during MIS 3. The flow variations did not follow the
474 Greenland temperature signal but rather aligned with the Antarctic temperature signal,
475 suggesting an ‘Antarctic’ influence on summer melting of the southern Laurentide Ice Sheet
476 (Hill et al., 2006). Particularly important was the Gulf of Mexico freshwater event that aligned in
477 time with the prominent Antarctic AIM warming episode during HS4. Taken together with the
478 data relating to flow of the Channel River, this implies that notable melting episodes took place
479 during HS1, HS2, HS3, and HS4 on the two main Northern Hemisphere mid-latitude ice sheets.
480 At the same times, the Southern Alps moraine record indicates retracted glaciers, further
481 highlighting the interhemispheric extent of warmer conditions during these four Heinrich
482 stadials. A similar illustration of Heinrich stadial warmth comes from pollen analysis of a core
483 from Lake Tulane in Florida (Grimm et al., 2006), not far from the site of the Gulf of Mexico
484 meltwater record obtained by Hill et al. (2006). The Lake Tulane core shows a succession of
485 peaks of *Pinus* pollen, indicating warm and wet summer climate episodes aligned with Heinrich
486 events 1-5 in the North Atlantic Ocean.

487

488 Another reinforcing example comes from a comprehensive glacier modelling experiment that
489 was unable to simulate the major fluctuations of the Alps icefields using forcing from the
490 Greenland temperature record from the GRIP ice core (Seguinot et al., 2018). Instead, the

491 requisite ice-volume fluctuations were best reproduced from a model forced by the Antarctic
492 temperature signal from the EPICA ice cores.

493

494 In regard to the second tenet, the Northern Hemisphere winter was an important linkage between
495 Greenland and European temperature changes during millennial-scale oscillations. The strength
496 of the monsoon in Asia tracked Greenland temperatures, with reduced northern subtropical
497 monsoonal circulation prevalent during Greenland stadials (Wang et al., 2001; Cheng et al.,
498 2016; Bradley and Diaz, 2021). The importance of the northern winter stadial arose from
499 meltwater-induced expanded sea ice on the North Atlantic Ocean that reduced the maritime
500 influence and imparted greater continentality to a huge expanse of the Northern Hemisphere
501 from northern North America to eastern Asia. The climate of this huge sector of the planet was
502 close to a critical winter threshold during the last glaciation, susceptible to perturbing triggers
503 such as episodes of warmer summers that injected glacial melt into the North Atlantic, with
504 effects including interpreted slowing of AMOC overturning, winter expansion of sea ice, and
505 extremely cold winters. The resulting episodes of strong seasonality required the existence of
506 large ice sheets to supply freshwater directly into the North Atlantic Ocean, and is why the
507 millennial-scale climate oscillations that produced winter stadial events were restricted to glacial
508 times.

509

510 By the Heinrich Summers hypothesis, differences in the amplitude and shape of the millennial-
511 scale climate oscillation signatures, as well as differences in the timing of climate breakpoints, in
512 the two polar hemispheres represent different responses to a common global climate signal. The
513 Antarctic response was a relatively smooth mean annual signal. The Greenland response

514 included a severe winter signal leveraged by the spread of sea ice on the North Atlantic. A reason
515 why the response may have been delayed and muted in Antarctica is that it may have depended
516 on disruption of Southern Ocean stratification and consequent ocean warming. Therefore, the
517 signals in the two polar regions could represent different responses to the same underlying global
518 summer warming episodes, with the north reacting more sharply and rapidly than the south.

519

520 Due to the post-glacial demise of the large northern ice sheets, no modern analog exists in the
521 North Atlantic region for a Heinrich-style influx of meltwater and icebergs leading to the
522 formation of extensive sea ice. But there are similarities to the situation caused by recent
523 Antarctic ice-sheet melt that has led to stratification of the adjacent parts of the Southern Ocean
524 and a spread of sea ice, resulting in subsurface ocean warming and surface ocean cooling in a
525 warming world (Bronselaer et al., 2018, 2020; Haumann et al., 2020).

526

527 The Heinrich Summers hypothesis is itself only a partial explanation for millennial-scale climate
528 oscillations because it does not account for what caused these climate changes of global
529 significance in the first place. A possible mechanism is encompassed in the Zealandia Switch
530 hypothesis, which proposes that shifts in Southern Hemisphere atmospheric and oceanic
531 circulation, interacting with southern continental platforms, had global climatic consequences
532 through direct linkages into tropical circulation systems (Denton et al., 2021). The temporal
533 commonality of glacier-related records at southern and northern mid-latitude localities of New
534 Zealand and the Channel River in western Europe, along with melting of sectors of northern ice
535 bodies during Heinrich episodes, could reflect changes in the latitude and strength of the austral
536 wind system, with the far-reaching climate consequences. The overall implication is that the

537 austral westerlies could have worked together with the planet's heat engine in the tropical ocean
538 to produce the global footprint necessary for the climate oscillations superimposed on the last
539 glaciation and its termination.

540

541 Comprehensive tests of the Heinrich Summers hypothesis rely on quantifying seasonal
542 conditions from robust paleo-proxy chronologies in both polar hemispheres. The emerging
543 evidence from temperature-sensitive glaciers located in opposite polar hemispheres that
544 apparently advanced and retreated in synchrony on millennial timescales during the last
545 glaciation, along with the in-phase ice-age termination, argues for the necessity of a modified
546 unifying theory for Quaternary glaciations and global climate change.

547

548

549 **Acknowledgements**

550

551 Research in the Southern Alps of New Zealand was supported by the National Science
552 Foundation, the Comer Family Foundation, and the Quesada Family Foundation. ST was
553 supported by IFREMER 'Marine Geosciences' funding, and the MAOREE project from the
554 LEFE-IMAGO (CNRS-INSU) research program. AEP was supported by a National Science
555 Foundation CAREER Award (no. 1554990). DJAB was supported by the GNS Science 'Global
556 Change through Time' research program, via the New Zealand Government's Strategic Science
557 Investment Fund. We thank the reviewers for their constructive comments, which improved the
558 manuscript.

559

560
561
562
563
564
565
566
567
568
569
570
571
572
573
574
575
576
577
578
579
580
581
582
583
584
585
586
587
588
589
590
591
592
593
594
595
596
597
598
599
600
601
602
603
604
605

REFERENCES

- Ammann, B., von Grafenstein, U., van Raden, U.J., 2013. Biotic responses to rapid warming about 14,685 yr BP: Introduction to a case study at Gerzensee (Switzerland). *Palaeogeography, Palaeoclimatology, Palaeoecology* 391, 3-12.
- Andersen, K.K., Azuma, N., Barnola, J.M., Bigler, M., Biscaye, P., Caillon, N., Chappellaz, J., Clausen, H.B., Dahl-Jensen, D., Fischer, H., Flückiger, J., Fritzsche, D., Fujii, Y., Goto-Azuma, K., Grønvold, K., Gundestrup, N.S., Hansson, M., Huber, C., Hvidberg, C.S., Johnsen, S.J., Jonsell, U., Jouzel, J., Kipfstuhl, S., Landais, A., Leuenberger, M., Lorrain, R., Masson-Delmotte, V., Miller, H., Motoyama, H., Narita, H., Popp, T., Rasmussen, S.O., Raynaud, D., Rothlisberger, R., Ruth, U., Samyn, D., Schwander, J., Shoji, H., Siggard-Andersen, M.L., Steffensen, J.P., Stocker, T., Sveinbjörnsdóttir, A.E., Svensson, A., Takata, M., Tison, J.L., Thorsteinsson, T., Watanabe, O., Wilhelms, F., White, J.W.C., North Greenland Ice Core Project, m., 2004. High-resolution record of Northern Hemisphere climate extending into the last interglacial period. *Nature* 431, 147-151.
- Anderson, B., 2005. Interactive comment on "Synoptic climate change as a driver of late Quaternary glaciations in the mid-latitudes of the Southern Hemisphere" by H. Rother and J. Shulmeister. *Climate of the Past Discussions* 1, S161-S167.
- Anderson, B., Lawson, W., Owens, I., Goodsell, B., 2006. Past and future mass balance of 'Ka Roimata o Hine Hukatere' Franz Josef Glacier, New Zealand. *Journal of Glaciology* 52, 597-607.
- Anderson, B., Mackintosh, A., 2006. Temperature change is the major driver of late-glacial and Holocene glacier fluctuations in New Zealand. *Geology* 34, 121-124.
- Anderson, B., Mackintosh, A., 2012. Controls on mass balance sensitivity of maritime glaciers in the Southern Alps, New Zealand: The role of debris cover. *Journal of Geophysical Research* 117, F01003.
- Anderson, B., Mackintosh, A., Stumm, D., George, L., Kerr, T., Winter-Billington, A., Fitzsimons, S., 2010. Climate sensitivity of a high-precipitation glacier in New Zealand. *Journal of Glaciology* 56, 114-128.
- Atkinson, T.C., Briffa, K.R., Coope, G.R., 1987. Seasonal temperatures in Britain during the past 22,000 years, reconstructed using beetle remains. *Nature* 325, 587-592.
- Barker, S., Chen, J., Gong, X., Jonkers, L., Knorr, G., Thornalley, D., 2015. Icebergs not the trigger for North Atlantic cold events. *Nature* 520, 333-336.
- Barker, S., Knorr, G., 2007. Antarctic climate signature in the Greenland ice core record. *Proceedings of the National Academy of Sciences* 104, 17278-17282.

606 Barrell, D.J.A., Andersen, B.G., Denton, G.H., 2011. Glacial geomorphology of the central
607 South Island, New Zealand. GNS Science Monograph 27, 81 pp.
608

609 Böhm, E., Lippold, J., Gutjahr, M., Frank, M., Blaser, P., Antz, B., Fohlmeister, J., Frank, N.,
610 Andersen, M.B., Deininger, M., 2015. Strong and deep Atlantic meridional overturning
611 circulation during the last glacial cycle. *Nature* 517, 73-76.
612

613 Boswell, S.M., Toucanne, S., Pitel-Roudaut, M., Creyts, T.T., Eynaud, F., Bayon, G., 2019.
614 Enhanced surface melting of the Fennoscandian Ice Sheet during periods of North Atlantic
615 cooling. *Geology* 47, 664-668.
616

617 Bradley, R. S., & Diaz, H. F., 2021. Late Quaternary abrupt climate change in the tropics and
618 sub- tropics: The continental signal of tropical hydroclimatic events (THEs). *Reviews of*
619 *Geophysics* 59(4), e2020RG000732.
620

621 Broecker, W.S., 1998. Paleocean circulation during the last deglaciation: A bipolar seesaw?
622 *Paleoceanography* 13, 119-121.
623

624 Broecker, W.S., 2006. Abrupt climate change revisited. *Global and Planetary Change* 54, 211-
625 215.
626

627 Bromley, G., Putnam, A., Borns, H., Lowell, T., Sandford, T., Barrell, D., 2018. Interstadial rise
628 and younger dryas demise of Scotland's last ice fields. *Paleoceanography and Paleoclimatology*
629 33, 412-429.
630

631 Bromley, G.R.M., Putnam, A.E., Rademaker, K.M., Lowell, T.V., Schaefer, J.M., Hall, B.L.,
632 Winckler, G., Birkel, S.D., Borns, H.W., 2014. Younger Dryas deglaciation of Scotland driven
633 by warming summers. *Proceedings of the National Academy of Sciences* 111, 6215-6219.
634

635 Bronselaer, B., Russell, J.L., Winton, M., Williams, N.L., Key, R.M., Dunne, J.P., Feely, R.A.,
636 Johnson, K.S., Sarmiento, J.L., 2020. Importance of wind and meltwater for observed chemical
637 and physical changes in the Southern Ocean. *Nature Geoscience* 13, 35-42.
638

639 Bronselaer, B., Winton, M., Griffies, S.M., Hurlin, W.J., Rodgers, K.B., Sergienko, O.V.,
640 Stouffer, R.J., Russell, J.L., 2018. Change in future climate due to Antarctic meltwater. *Nature*
641 564, 53-58.
642

643 Buizert, C., Cuffey, K.M., Severinghaus, J.P., Baggenstos, D., Fudge, T.J., Steig, E.J., Markle,
644 B.R., Winstrup, M., Rhodes, R.H., Brook, E.J., Sowers, T.A., Clow, G.D., Cheng, H., Edwards,
645 R.L., Sigl, M., McConnell, J.R., Taylor, K.C., 2015. The WAIS Divide deep ice core WD2014
646 chronology — Part 1: Methane synchronization (68-31 ka BP) and the gas age-ice age
647 difference. *Climate of the Past* 11, 153-173.
648

649 Buizert, C., Gkinis, V., Severinghaus, J.P., He, F., Lacavalier, B.S., Kindler, P., Leuenberger,
650 M., Carlson, A.E., Vinther, B., Masson-Delmotte, V., White, J.W.C., Liu, Z., Otto-Bliesner, B.,

651 Brook, E.J., 2014. Greenland temperature response to climate forcing during the last
652 deglaciation. *Science* 345, 1177-1180.
653
654 Buizert, C., Keisling, B.A., Box, J.E., He, F., Carlson, A.E., Sinclair, G., DeConto, R.M., 2018.
655 Greenland- wide seasonal temperatures during the last deglaciation. *Geophysical Research*
656 *Letters* 45, 1905-1914.
657
658 Burga, C.A., 1988. Swiss vegetation history during the last 18 000 years. *New Phytologist* 110,
659 581-602.
660
661 Cheng, H., Edwards, R.L., Sinha, A., Spötl, C., Yi, L., Chen, S., Kelly, M., Kathayat, G., Wang,
662 X., Li, X., Kong, X., Wang, Y., Ning, Y., Zhang, H., 2016. The Asian monsoon over the past
663 640,000 years and ice age terminations. *Nature* 534, 640-646.
664
665 Clark, P.U., Mix, A.C., 2002. Ice sheets and sea level of the Last Glacial Maximum. *Quaternary*
666 *Science Reviews* 21, 1-7.
667
668 Clark, P.U., Dyke, A.S., Shakun, J.D., Carlson, A.E., Clark, J., Wohlfarth, B., Mitrovica, J.X.,
669 Hostetler, S.W., McCabe, A.M., 2009. The last glacial maximum. *Science* 325, 710-714.

670 Crowley, T.J., 1992. North Atlantic deep water cools the Southern Hemisphere.
671 *Paleoceanography* 7, 489-497.
672
673 Cuffey, K.M., Clow, G.D., Steig, E.J., Buizert, C., Fudge, T.J., Koutnik, M., Waddington, E.D.,
674 Alley, R.B., Severinghaus, J.P., 2016. Deglacial temperature history of West Antarctica.
675 *Proceedings of the National Academy of Sciences* 113, 14249-14254.
676
677 Daly, C., Widrlechner, M.P., Halbleib, M.D., Smith, J.I., Gibson, W.P., 2012. Development of a
678 new USDA plant hardiness zone map for the United States. *Journal of Applied Meteorology and*
679 *Climatology* 51, 242-264.
680
681 Denton, G.H., Alley, R.B., Comer, G.C., Broecker, W.S., 2005. The role of seasonality in abrupt
682 climate change. *Quaternary Science Reviews* 24, 1159-1182.
683
684 Denton, G.H., Putnam, A.E., Russell, J.L., Barrell, D.J.A., Schaefer, J.M., Kaplan, M.R., Strand,
685 P.D., 2021. The Zealandia Switch: Ice age climate shifts viewed from Southern Hemisphere
686 moraines. *Quaternary Science Reviews* 257, 106771.
687
688 Doughty, A.M., Schaefer, J.M., Denton, G.H., Kaplan, M.R., Putnam, A.E., Andersen, B.G.,
689 Barrell, D.J.A., Schwartz, R., Finkel, R.C., 2015. Mismatch of glacier extent and summer
690 insolation in Southern Hemisphere mid-latitudes. *Geology* 43, 407-410.
691
692 Eicher, U., Siegenthaler, U., 1976. Palynological and oxygen isotope investigations on Late-
693 Glacial sediment cores from Swiss lakes. *Boreas* 5, 109-117.
694
695 Eynaud, F., Malaizé, B., Zaragosi, S., de Vernal, A., Scourse, J., Pujol, C., Cortijo, E., Grousset,
696 F.E., Penaud, A., Toucanne, S., Turon, J.-L., Auffret, G., 2012. New constraints on European

697 glacial freshwater releases to the North Atlantic Ocean. *Geophysical Research Letters* 39,
698 L15601.
699

700 Eynaud, F., Zaragosi, S., Scourse, J.D., Mojtahid, M., Bourillet, J.F., Hall, I.R., Penaud, A.,
701 Locascio, M., Reijonen, A., 2007. Deglacial laminated facies on the NW European continental
702 margin: The hydrographic significance of British-Irish Ice Sheet deglaciation and Fleuve
703 Manche paleoriver discharges. *Geochemistry, Geophysics, Geosystems* 8, Q06019.
704

705 Flückiger, J., Knutti, R., White, J.W.C., Renssen, H., 2008. Modeled seasonality of glacial abrupt
706 climate events. *Climate Dynamics* 31, 633-645.
707

708 Funder, S., Sørensen, A. H., Larsen, N. K., Bjørk, A. A., Briner, J. P., Olsen, J., Schomacker, A.,
709 Kjær, K. H., 2021. Younger Dryas ice margin retreat in Greenland: new evidence from
710 southwestern Greenland. *Climate of the Past* 17(2), 587-601.
711

712 Gibbard, P. L. (1988). The history of the great northwest European rivers during the past three
713 million years. *Philosophical Transactions of the Royal Society of London. B, Biological*
714 *Sciences*, 318(1191), 559-602.
715

716 Gil, I.M., Keigwin, L.D., Abrantes, F.G., 2009. Deglacial diatom productivity and surface ocean
717 properties over the Bermuda Rise, northeast Sargasso Sea. *Paleoceanography* 24, PA4101
718 doi:4110.1029/2008PA001729.
719

720 Grimm, E.C., Watts, W.A., Jacobson, G.L., Hansen, B.C.S., Almquist, H.R., Dieffenbacher-
721 Krall, A.C., 2006. Evidence for warm wet Heinrich events in Florida. *Quaternary Science*
722 *Reviews* 25, 2197-2211.
723

724 Guilderson, T.P., Allen, K., Landers, J.P., Ettwein, V.J., Cook, M.S., 2021. Can we better
725 constrain the timing of GNAIW/UNADW variability in the western equatorial Atlantic and its
726 relationship to climate change during the last deglaciation? *Paleoceanography and*
727 *Paleoclimatology* 36, e2020PA004187.
728

729 Haumann, F.A., Gruber, N., Münnich, M., 2020. Sea-ice induced Southern Ocean subsurface
730 warming and surface cooling in a warming climate. *AGU Advances* 1, e2019AV000132.
731

732 He, C., Liu, Z., Otto-Bliesner, B.L., Brady, E.C., Zhu, C., Tomas, R., Buizert, C., Severinghaus,
733 J.P., 2021. Abrupt Heinrich Stadial 1 cooling missing in Greenland oxygen isotopes. *Science*
734 *Advances* 7, eabh1007.
735

736 Henry, L.G., McManus, J.F., Curry, W.B., Roberts, N.L., Piotrowski, A.M., Keigwin, L.D.,
737 2016. North Atlantic ocean circulation and abrupt climate change during the last glaciation.
738 *Science* 353, 470-474.
739

740 Hill, H.W., Flower, B.P., Quinn, T.M., Hollander, D.J., Guilderson, T.P., 2006. Laurentide Ice
741 Sheet meltwater and abrupt climate change during the last glaciation. *Paleoceanography* 21,
742 PA1006.

743
744 Holland, D.M., Thomas, R.H., de Young, B., Ribergaard, M.H., Lyberth, B., 2008. Acceleration
745 of Jakobshavn Isbræ triggered by warm subsurface ocean waters. *Nature Geoscience* 1, 659-664.
746
747 Isarin, R.F.B., 1997. Permafrost distribution and temperatures in Europe during the Younger
748 Dryas. *Permafrost and Periglacial Processes* 8, 313-333.
749
750 Isarin, R.F.B., Bohncke, S.J.P., 1999. Mean July temperatures during the Younger Dryas in
751 northwestern and central Europe as inferred from climate indicator plant species. *Quaternary*
752 *Research* 51, 158-173.
753
754 Isarin, R.F.B., Renssen, H., Vandenberghe, J., 1998. The impact of the North Atlantic Ocean on
755 the Younger Dryas climate in northwestern and central Europe. *Journal of Quaternary Science*
756 13, 447-453.
757
758 Joughin, I., Shapero, D., Smith, B., Dutrieux, P., Barham, M., 2021. Ice-shelf retreat drives
759 recent Pine Island Glacier speedup. *Science Advances* 7, eabg3080.
760
761 Jouzel, J., Masson-Delmotte, V., Cattani, O., Dreyfus, G., Falourd, S., Hoffmann, G., Minster,
762 B., Nouet, J., Barnola, J.M., Chappellaz, J., Fischer, H., Gallet, J.C., Johnsen, S., Leuenberger,
763 M., Loulergue, L., Luethi, D., Oerter, H., Parrenin, F., Raisbeck, G., Raynaud, D., Schilt, A.,
764 Schwander, J., Selmo, E., Souchez, R., Spahni, R., Stauffer, B., Steffensen, J.P., Stenni, B.,
765 Stocker, T.F., Tison, J.L., Werner, M., Wolff, E.W., 2007. Orbital and millennial Antarctic
766 climate variability over the past 800,000 years. *Science* 317, 793-796.
767
768 Kaplan, M.R., Schaefer, J.M., Denton, G.H., Barrell, D.J.A., Chinn, T.J.H., Putnam, A.E.,
769 Andersen, B.G., Finkel, R.C., Schwartz, R., Doughty, A.M., 2010. Glacier retreat in New
770 Zealand during the Younger Dryas stadial. *Nature* 467, 194-197.
771
772 Kaplan, M.R., Schaefer, J.M., Denton, G.H., Doughty, A.M., Barrell, D.J.A., Chinn, T.J.H.,
773 Putnam, A.E., Andersen, B.G., Mackintosh, A., Finkel, R.C., Schwartz, R., Anderson, B., 2013.
774 The anatomy of long-term warming since 15 kyr ago in New Zealand based on net glacier
775 snowline rise. *Geology* 41, 887-890.
776
777 Kelley, S.E., Kaplan, M.R., Schaefer, J.M., Andersen, B.G., Barrell, D.J.A., Putnam, A.E.,
778 Denton, G.H., Schwartz, R., Finkel, R.C., Doughty, A.M., 2014. High-precision ¹⁰Be chronology
779 of moraines in the Southern Alps indicates synchronous cooling in Antarctica and New Zealand
780 42,000 years ago. *Earth and Planetary Science Letters* 405, 194-206.
781
782 Koffman, T.N.B., Schaefer, J.M., Putnam, A.E., Denton, G.H., Barrell, D.J.A., Rowan, A.V.,
783 Finkel, R.C., Rood, D.H., Schwartz, R., Plummer, M.A., Brocklehurst, S.H., 2017. A beryllium-
784 10 chronology of late-glacial moraines in the upper Rakaia valley, Southern Alps, New Zealand
785 supports Southern-Hemisphere warming during the Younger Dryas. *Quaternary Science Reviews*
786 170, 14-25.
787

788 Levy, L.B., Kelly, M.A., Lowell, T.V., Hall, B.L., Howley, J.A., Smith, C.A., 2016. Coeval
789 fluctuations of the Greenland ice sheet and a local glacier, central East Greenland, during late
790 glacial and early Holocene time. *Geophysical Research Letters* 43, 1623-1631.
791

792 Li, C., Battisti, D.S., Schrag, D.P., Tziperman, E., 2005. Abrupt climate shifts in Greenland due
793 to displacements of the sea ice edge. *Geophysical Research Letters* 32, L19702.
794

795 Lorrey, A., Fauchereau, N., Stanton, C., Chappell, P., Phipps, S., Mackintosh, A., Renwick, J.,
796 Goodwin, I., Fowler, A., 2014. The Little Ice Age climate of New Zealand reconstructed from
797 Southern Alps cirque glaciers: a synoptic type approach. *Climate Dynamics* 42, 3039-3060.
798

799 Marcott, S.A., Clark, P.U., Padman, L., Klinkhammer, G.P., Springer, S.R., Liu, Z., Otto-
800 Bliesner, B.L., Carlson, A.E., Ungerer, A., Padman, J., He, F., Cheng, J., Schmittner, A., 2011.
801 Ice-shelf collapse from subsurface warming as a trigger for Heinrich events. *Proceedings of the*
802 *National Academy of Sciences* 108, 13415-13419.
803

804 Martinez-Lamas, R., Toucanne, S., S., Debret, M., Riboulot, V., Deloffre, J., Boissier, A.,
805 Cheron, S., Pitel, M., Bayon, G., Giosan, L., Soulet, G., 2020. Linking Danube River activity to
806 alpine ice-sheet fluctuations during the last glacial (ca. 33–17 ka BP): Insights into the
807 continental signature of Heinrich Stadials. *Quaternary Science Reviews* 229, 106136.
808

809 Ménot, G., Bard, E., Rostek, F., Weijers, J.W.H., Hopmans, E.C., Schouten, S., Damste, J.S.S.,
810 2006. Early reactivation of European rivers during the last deglaciation. *Science* 313, 1623-1625.
811

812 Naafs, B.D.A., Hefter, J., Grützner, J., Stein, R., 2013. Warming of surface waters in the mid-
813 latitude North Atlantic during Heinrich events. *Paleoceanography* 28, 153-163.
814

815 Pahnke, K., Zahn, R., 2005. Southern Hemisphere water mass conversion linked with North
816 Atlantic climate variability. *Science* 307, 1741-1746.
817

818 Peck, V.L., Hall, I.R., Zahn, R., Elderfield, H., 2008. Millennial-scale surface and subsurface
819 paleothermometry from the northeast Atlantic, 55–8 ka BP. *Paleoceanography* 23, PA3221.
820

821 Pedro, J.B., Jochum, M., Buizert, C., He, F., Barker, S., Rasmussen, S.O., 2018. Beyond the
822 bipolar seesaw: Toward a process understanding of interhemispheric coupling. *Quaternary*
823 *Science Reviews* 192, 27-46.
824

825 Pedro, J.B., van Ommen, T.D., Rasmussen, S.O., Morgan, V.I., Chappellaz, J., Moy, A.D.,
826 Masson-Delmotte, V., Delmotte, M., 2011. The last deglaciation: timing the bipolar seesaw.
827 *Clim. Past* 7, 671-683.
828

829 Purdie, H., Anderson, B., Chinn, T., Owens, I., Mackintosh, A., Lawson, W., 2014. Franz Josef
830 and Fox Glaciers, New Zealand: Historic length records. *Global and Planetary Change* 121, 41-
831 52.
832

833 Putnam, A.E., Denton, G.H., Schaefer, J.M., Barrell, D.J.A., Andersen, B.G., Finkel, R.,
834 Schwartz, R., Doughty, A.M., Kaplan, M., Schlüchter, C., 2010a. Glacier advance in southern
835 middle latitudes during the Antarctic Cold Reversal. *Nature Geoscience* 3, 700-704.
836

837 Putnam, A.E., Schaefer, J.M., Barrell, D.J.A., Vandergoes, M., Denton, G.H., Kaplan, M.R.,
838 Schwartz, R., Finkel, R.C., Goehring, B.M., Kelley, S.E., 2010b. In situ cosmogenic ^{10}Be
839 production-rate calibration from the Southern Alps, New Zealand. *Quaternary Geochronology* 5,
840 392-409.
841

842 Putnam, A.E., Schaefer, J.M., Denton, G.H., Barrell, D.J.A., Andersen, B.G., Koffman, T.N.B.,
843 Rowan, A.V., Finkel, R.C., Rood, D.H., Schwartz, R., Vandergoes, M.J., Plummer, M.A.,
844 Brocklehurst, S.H., Kelley, S.E., Ladig, K.L., 2013a. Warming and glacier recession in the
845 Rakaia valley, Southern Alps of New Zealand, during Heinrich Stadial 1. *Earth and Planetary*
846 *Science Letters* 382, 98-110.
847

848 Putnam, A.E., Schaefer, J.M., Denton, G.H., Barrell, D.J.A., Birkel, S.D., Andersen, B.G.,
849 Kaplan, M.R., Finkel, R.C., Schwartz, R., Doughty, A.M., 2013b. The Last Glacial Maximum at
850 44°S documented by a ^{10}Be moraine chronology at Lake Ohau, Southern Alps of New Zealand.
851 *Quaternary Science Reviews* 62, 114-141.
852

853 Putnam, A.E., Schaefer, J.M., Denton, G.H., Barrell, D.J.A., Finkel, R.C., Andersen, B.G.,
854 Schwartz, R., Chinn, T.J.H., Doughty, A.M., 2012. Regional climate control of glaciers in New
855 Zealand and Europe during the pre-industrial Holocene. *Nature Geoscience* 5, 627-630.
856

857 Rashid, H., Saint-Ange, F., Barber, D. C., Smith, M. E., Devalia, N., 2012. Fine scale sediment
858 structure and geochemical signature between eastern and western North Atlantic during Heinrich
859 events 1 and 2. *Quaternary Science Reviews* 46, 136-150.
860

861 Rasmussen, S.O., Bigler, M., Blockley, S.P., Blunier, T., Buchardt, S.L., Clausen, H.B.,
862 Cvijanovic, I., Dahl-Jensen, D., Johnsen, S.J., Fischer, H., Gkinis, V., Guillevic, M., Hoek, W.Z.,
863 Lowe, J.J., Pedro, J.B., Popp, T., Seierstad, I.K., Steffensen, J.P., Svensson, A.M., Vellelonga,
864 P., Vinther, B.M., Walker, M.J.C., Wheatley, J.J., Winstrup, M., 2014. A stratigraphic
865 framework for abrupt climatic changes during the Last Glacial period based on the three
866 synchronized Greenland ice-core records: refining and extending the INTIMATE even
867 stratigraphy. *Quaternary Science Reviews* 106, 14-28.
868

869 Rasmussen, S.O., Andersen, K.K., Svensson, A.M., Steffensen, J.P., Vinther, B.M., Clausen,
870 H.B., Siggaard-Andersen, M.-L., Johnsen, S.J., Larsen, L.B., Dahl-Jensen, D., Bigler, M.,
871 Röthlisberger, R., Fischer, H., Goto-Azuma, K., Hansson, M.E., Ruth, U., 2006. A new
872 Greenland ice core chronology for the last glacial termination. *Journal of Geophysical Research*
873 111, D06102.
874

875 Rasmussen, T.L., Thomsen, E., 2004. The role of the North Atlantic Drift in the millennial
876 timescale glacial climate fluctuations. *Palaeogeography, Palaeoclimatology, Palaeoecology* 210,
877 101-116.
878

879 Rasmussen, T.L., Thomsen, E., 2008. Warm Atlantic surface water inflow to the Nordic seas 34–
880 10 calibrated ka B.P. *Paleoceanography* 23, PA1201.
881

882 Rasmussen, T.L., Thomsen, E., Moros, M., 2016. North Atlantic warming during Dansgaard-
883 Oeschger events synchronous with Antarctic warming and out-of-phase with Greenland climate.
884 *Scientific Reports* 6, 20535.
885

886 Renssen, H., Bogaart, P.W., 2003. Atmospheric variability over the ~14.7 kyr BP stadial-
887 interstadial transition in the North Atlantic region as simulated by an AGCM. *Climate Dynamics*
888 20, 301-313.
889

890 Renssen, H., Isarin, R.F.B., 2001. The two major warming phases of the last deglaciation at
891 ~14.7 and ~11.5 ka cal BP in Europe: climate reconstructions and AGCM experiments. *Global*
892 *and Planetary Change* 30, 117-153.
893

894 Roberts, W.H.G., Hopcroft, P.O., 2020. Controls on the tropical response to abrupt climate
895 changes. *Geophysical Research Letters* 47, e2020GL087518.
896

897 Ruhlemann, C., Mulitza, S., Muller, P.J., Wefer, G., Zahn, R., 1999. Warming of the tropical
898 Atlantic Ocean and slowdown of thermohaline circulation during the last deglaciation. *Nature*
899 402, 511-514.
900

901 Sánchez Goñi, M., Cacho, I., Turon, J., Guiot, J., Sierro, F., Peyrouquet, J., Grimalt, J.,
902 Shackleton, N., 2002. Synchronicity between marine and terrestrial responses to millennial scale
903 climatic variability during the last glacial period in the Mediterranean region. *Climate Dynamics*
904 19, 95-105.
905

906 Sánchez Goñi, M.a.F., Turon, J.-L., Eynaud, F., Gendreau, S., 2000. European climatic response
907 to millennial-scale changes in the atmosphere–ocean system during the Last Glacial Period.
908 *Quaternary Research* 54, 394-403.
909

910 Schaefer, J.M., Denton, G.H., Barrell, D.J.A., Ivy-Ochs, S., Kubik, P.W., Andersen, B.G.,
911 Phillips, F.M., Lowell, T.V., Schluchter, C., 2006. Near-synchronous interhemispheric
912 termination of the Last Glacial Maximum in mid-latitudes. *Science* 312, 1510-1513.
913

914 Schaefer, J.M., Denton, G.H., Kaplan, M., Putnam, A., Finkel, R.C., Barrell, D.J.A., Andersen,
915 B.G., Schwartz, R., Mackintosh, A., Chinn, T., Schlüchter, C., 2009. High-frequency Holocene
916 glacier fluctuations in New Zealand differ from the northern signature. *Science* 324, 622-625.
917

918 Schaefer, J.M., Putnam, A.E., Denton, G.H., Kaplan, M.R., Birkel, S.D., Doughty, A.M., Kelley,
919 S.E., Barrell, D.J.A., Finkel, R.C., Winckler, G., Anderson, R.F., Ninnemann, U.S., Barker, S.,
920 Schwartz, R., Schluichter, C., 2015. The Southern Glacial Maximum 65,000 years ago and its
921 unfinished Termination. *Quaternary Science Reviews* 114, 52-60.
922

923 Schenk, F., Väiliranta, M., Muschitiello, F., Tarasov, L., Heikkilä, M., Björck, S., Brandefelt, J.,
924 Johansson, A.V., Näslund, J.-O., Wohlfarth, B., 2018. Warm summers during the Younger Dryas
925 cold reversal. *Nature Communications* 9, 1634.
926

927 Seguinot, J., Ivy-Ochs, S., Jouvét, G., Huss, M., Funk, M., Preusser, F., 2018. Modelling last
928 glacial cycle ice dynamics in the Alps. *The Cryosphere* 12, 3265-3285.
929

930 Severinghaus, J.P., Sowers, T., Brook, E.J., Alley, R.B., Bender, M.L., 1998. Timing of abrupt
931 climate change at the end of the Younger Dryas interval from thermally fractionated gases in
932 polar ice. *Nature* 391, 141-146.
933

934 Shackleton, N.J., Hall, M.A., Vincent, E., 2000. Phase relationships between millennial-scale
935 events 64,000- 24,000 years ago. *Paleoceanography* 15, 565-569.
936

937 Shaffer, G., Olsen, S.M., Bjerrum, C.J., 2004. Ocean subsurface warming as a mechanism for
938 coupling Dansgaard-Oeschger climate cycles and ice-rafting events. *Geophysical Research*
939 *Letters* 31, L24202.

940

941 Siegenthaler, U., Eicher, U., Oeschger, H., Dansgaard, W., 1984. Lake sediments as continental
942 $\delta^{18}\text{O}$ records from the glacial/post-glacial transition. *Annals of Glaciology* 5, 149-152.
943

944 Sime, L.C., Hopcroft, P.O., Rhodes, R.H., 2019. Impact of abrupt sea ice loss on Greenland
945 water isotopes during the last glacial period. *Proceedings of the National Academy of Sciences*
946 116, 4099-4104.
947

948 Schneider, R., Schmitt, J., Köhler, P., Joos, F., & Fischer, H., 2013. A reconstruction of
949 atmospheric carbon dioxide and its stable carbon isotopic composition from the penultimate
950 glacial maximum to the last glacial inception. *Climate of the Past* 9, 2507-2523.
951

952 Steig, E.J., Alley, R.B., 2002. Phase relationships between Antarctic and Greenland climate
953 records. *Annals of Glaciology* 35, 451-456.
954

955 Steig, E.J., Jones, T.R., Schauer, A.J., Kahle, E.C., Morris, V.A., Vaughn, B.H., Davidge, L.,
956 White, J.W.C., 2021. Continuous-flow analysis of $\delta^{17}\text{O}$, $\delta^{18}\text{O}$, and δD of H_2O on an ice core
957 from the South Pole. *Frontiers in Earth Science* 9, 640292.
958

959 Stern, J.V., Lisiecki, L.E., 2013. North Atlantic circulation and reservoir age changes over the
960 past 41,000 years. *Geophysical Research Letters* 40, 3693-3697.
961

962 Stocker, T.F., Johnsen, S.J., 2003. A minimum thermodynamic model for the bipolar seesaw.
963 *Paleoceanography* 18, 1087.
964

965 Strand, P.D., Schaefer, J.M., Putnam, A.E., Denton, G.H., Barrell, D.J.A., Koffman, T.N.B.,
966 Schwartz, R., 2019. Millennial-scale pulsebeat of glaciation in the Southern Alps of New
967 Zealand. *Quaternary Science Reviews* 220, 165-177.
968

969 Svensson, A., Andersen, K.K., Bigler, M., Clausen, H.B., Dahl-Jensen, D., Davies, S.M.,
970 Johnsen, S.J., Muscheler, R., Parrenin, F., Rasmussen, S.O., Röthlisberger, R., Seierstad, I.,
971 Steffensen, J.P., Vinther, B.M., 2008. A 60 000 year Greenland stratigraphic ice core
972 chronology. *Clim. Past* 4, 47-57.
973
974 Su, Z., Ingersoll, A.P., He, F., 2016. On the abruptness of Bølling–Allerød warming. *Journal of*
975 *Climate* 29, 4965-4975.
976
977 Thiagarajan, N., Subhas, A.V., Southon, J.R., Eiler, J.M., Adkins, J.F., 2014. Abrupt pre-
978 Bolling-Allerod warming and circulation changes in the deep ocean. *Nature* 511, 75-78.
979
980 Toucanne, S., Soulet, G., Freslon, N., Silva Jacinto, R., Dennielou, B., Zaragosi, S., Eynaud, F.,
981 Bourillet, J.-F., Bayon, G., 2015. Millennial-scale fluctuations of the European Ice Sheet at the
982 end of the last glacial, and their potential impact on global climate. *Quaternary Science Reviews*
983 123, 113-133.
984
985 Toucanne, S., Zaragosi, S., Bourillet, J.-F., Marieu, V., Cremer, M., Kageyama, M., Van Vliet-
986 Lanoë, B., Eynaud, F., Turon, J.-L., Gibbard, P.L., 2010. The first estimation of Fleuve Manche
987 paleoriver discharge during the last deglaciation: Evidence for Fennoscandian ice sheet
988 meltwater flow in the English Channel ca 20-18 ka ago. *Earth and Planetary Science Letters* 290,
989 459-473.
990
991 Toucanne, S., Zaragosi, S., Bourillet, J.F., Cremer, M., Eynaud, F., Van Vliet-Lanoë, B., Penaud,
992 A., Fontanier, C., Turon, J.L., Cortijo, E., Gibbard, P.L., 2009. Timing of massive 'Fleuve
993 Manche' discharges over the last 350 kyr: insights into the European ice-sheet oscillations and
994 the European drainage network from MIS 10 to 2. *Quaternary Science Reviews* 28, 1238-1256.
995
996 van Raden, U.J., Colombaroli, D., Gilli, A., Schwander, J., Bernasconi, S.M., van Leeuwen, J.,
997 Leuenberger, M., Eicher, U., 2013. High-resolution late-glacial chronology for the Gerzensee
998 lake record (Switzerland): $\delta^{18}\text{O}$ correlation between a Gerzensee-stack and NGRIP.
999 *Palaeogeography, Palaeoclimatology, Palaeoecology* 391, 13-24.
1000
1001 WAIS Divide Project Members, 2015. Precise inter-polar phasing of abrupt climate change
1002 during the last ice age. *Nature* 520, 661-665.
1003
1004 Walczak, M.H., Mix, A.C., Cowan, E.A., Fallon, S., Fifield, L.K., Alder, J.R., Du, J., Haley, B.,
1005 Hobern, T., Padman, J., Praetorius, S.K., Schmittner, A., Stoner, J.S., Zellers, S.D., 2020.
1006 Phasing of millennial-scale climate variability in the Pacific and Atlantic Oceans. *Science* 370,
1007 716-720.
1008
1009 Wang, Y.J., Cheng, H., Edwards, R.L., An, Z.S., Wu, J.Y., Shen, C.C., Dorale, J.A., 2001. A
1010 high-resolution absolute-dated Late Pleistocene monsoon record from Hulu Cave, China. *Science*
1011 294, 2345-2348.

1012 Winski, D. A., Fudge, T. J., Ferris, D. G., Osterberg, E. C., Fegyveresi, J. M., Cole-Dai, J., ... &
1013 McConnell, J. R., 2019. The SP19 chronology for the South Pole Ice Core–Part 1: volcanic
1014 matching and annual layer counting. *Climate of the Past* 15, 1793-1808.

1015
1016 Wittmeier, H.E., Schaefer, J.M., Bakke, J., Rupper, S., Paasche, Ø., Schwartz, R., Finkel, R.C.,
1017 2020. Late Glacial mountain glacier culmination in Arctic Norway prior to the Younger Dryas.
1018 Quaternary Science Reviews 245, 106461.
1019
1020 Zaragosi, S., Eynaud, F., Pujol, C., Auffret, G.A., Turon, J.-L., Garlan, T., 2001. Initiation of the
1021 European deglaciation as recorded in the northwestern Bay of Biscaye slope environments
1022 (Meriadzek Terrace and Trevelyan Escarpment): a multi-proxy approach. Earth and Planetary
1023 Science Letters 188, 493-507.
1024
1025 Zhou, Y., McManus, J. F., Jacobel, A. W., Costa, K. M., Wang, S., Caraveo, B. A., 2021.
1026 Enhanced iceberg discharge in the western North Atlantic during all Heinrich events of the last
1027 glaciation. Earth and Planetary Science Letters 564, 116910.
1028

1029
1030
1031
1032
1033
1034
1035
1036
1037
1038
1039
1040
1041
1042
1043
1044
1045
1046
1047
1048
1049
1050
1051
1052
1053
1054
1055
1056
1057
1058
1059
1060
1061
1062
1063
1064
1065
1066
1067
1068
1069
1070
1071
1072
1073
1074

Figure Captions

Figure 1. Superimposition of Greenland (blue; NGRIP; Andersen et al., 2004; Buizert et al., 2015) and Antarctic (orange, WDC; Buizert et al., 2015) ice-core $\delta^{18}\text{O}$ records. Panels show ice-core signatures spanning 22 – 68 ka (a); 10 – 26 ka, i.e., including deglacial time (b); and enlargements of the 34 – 41 ka (c) and 43 – 51 ka (d) time intervals, including the HS4 and HS5 stadials, respectively. HS: Heinrich stadial. GI: Greenland interstadials. GIs are numbered according to Rasmussen et al. (2006, 2014) and Buizert et al. (2015). Light blue/orange lines correspond to high-resolution data from the NGRIP and WDC ice cores, respectively. Thick blue/orange lines are 50-pt moving averages (from Buizert et al., 2015). Downward-pointing black arrows signify intervals of coeval Greenland and Antarctic cooling during Greenland interstadials. Vertical pink bands show Heinrich stadials. Vertical gray bands show Greenland interstadials. Figure adapted from Buizert et al. (2015).

Figure 2: Palaeogeography of western Europe at the Last Glacial Maximum. The glacial limits of the western European Ice Sheet (EIS), including the Scandinavian (SIS), British-Irish (BIIS) components, and Alpine Ice Sheet (AIS) are shown, along with the Channel and Danube river hydrographic networks (white arrows). Br.: Brandenburg-Leszno moraine (formed between 23.4 ± 0.3 and 20.3 ± 0.2 ka), Fr.: Frankfurt-Poznan moraine (from 18.7 ± 0.3 to 18.2 ± 0.2 ka), Pm.: Pomeranian moraine (from 16.7 ± 0.2 to 15.7 ± 0.3 ka) (Toucanne et al., 2015). The location of core MD95-2002 in the Bay of Biscay is also shown.

Figure 3. Comparison of a) Meltwater flux through the Channel River (Toucanne et al., 2015) with b) intervals of moraine construction in the Southern Alps of New Zealand (Denton et al., 2021, and references therein). In (a), the XRF Fe/Ca (light blue) and Ti/Ca (red) ratios from core MD95-2002 (see location in Figure 2) can be regarded as a first-order indication of relative changes in the amount of fine terrigenous components of Baltic origin from the Channel River. The latter is independently supported by the logarithmic plot of turbidite flux (dark blue) in the deep Bay of Biscay, a proxy for Channel River floods (Toucanne et al., 2015). Vertical pink bands correspond to Heinrich stadials (HS) and vertical blue bands are intervals of reduced runoff from the Channel River. LLGM refers to the local last glacial maximum. R1 – R5 refers to the Channel River meltwater (i.e., runoff) intervals identified by Toucanne et al. (2015). (b), episodes of Southern Alps moraine construction correspond with periods of reduced meltwater flux into the North Atlantic, whereas periods of Southern Alps glacier recession (such as during Heinrich Stadial 1) coincide with periods of intensified meltwater discharge into the Bay of Biscay. The moraine age versus temperature plot in Figure 3 is based on data from Table S-2 in Denton et al. (2021).

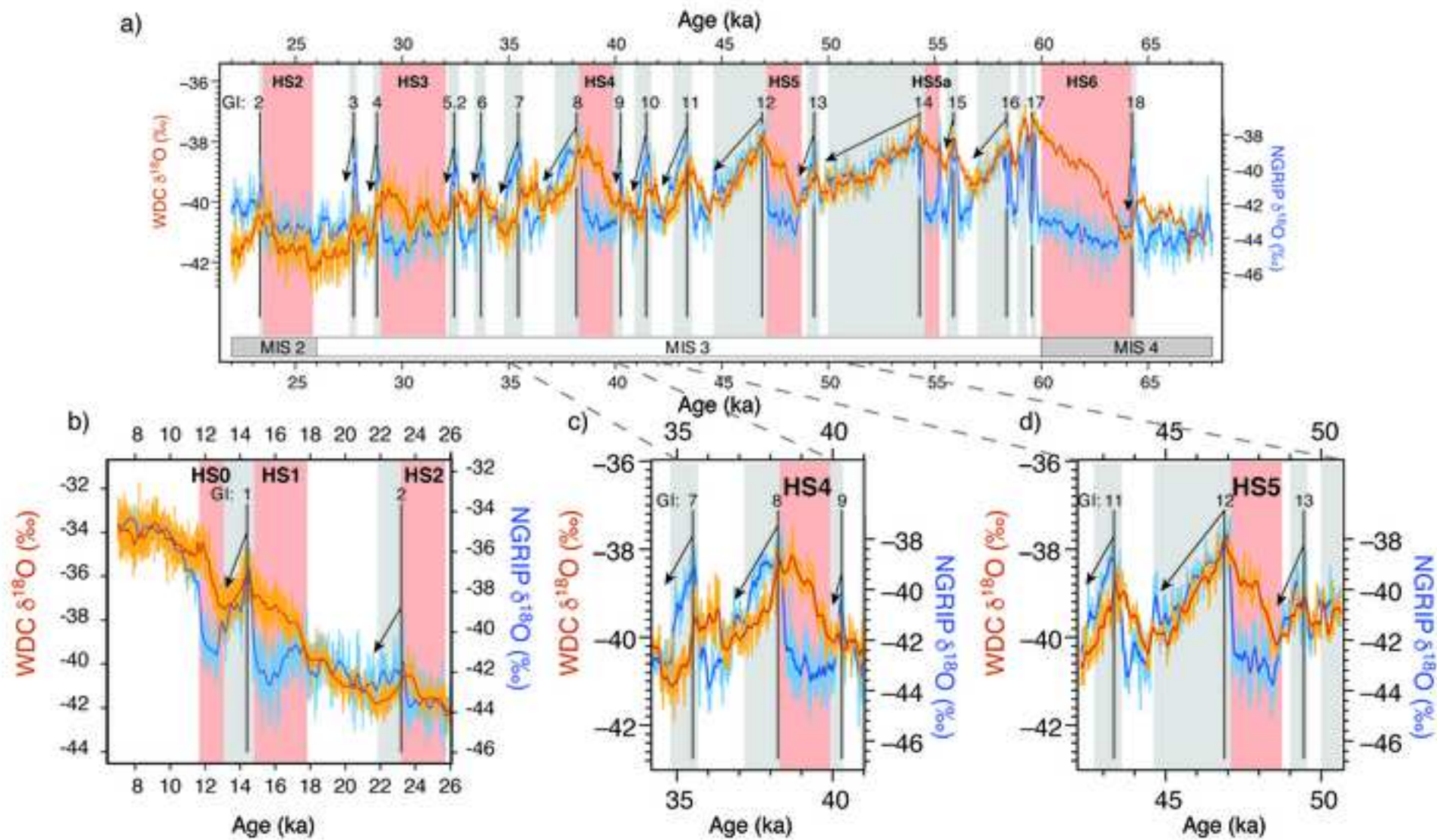
Figure 4. Oblique aerial photograph, vantage north, of the left-lateral moraine system deposited by the former Pukaki Glacier during the last glaciation, which flowed southward from the Main Divide of the Southern Alps. Exposure dates of these moraines are included in Figure 3, with details given in Kelley et al. (2014), Doughty et al. (2015), Strand et al. (2019), and Denton et al. (2021). Maps providing broader geographical context for these specific field areas are also presented in these studies.

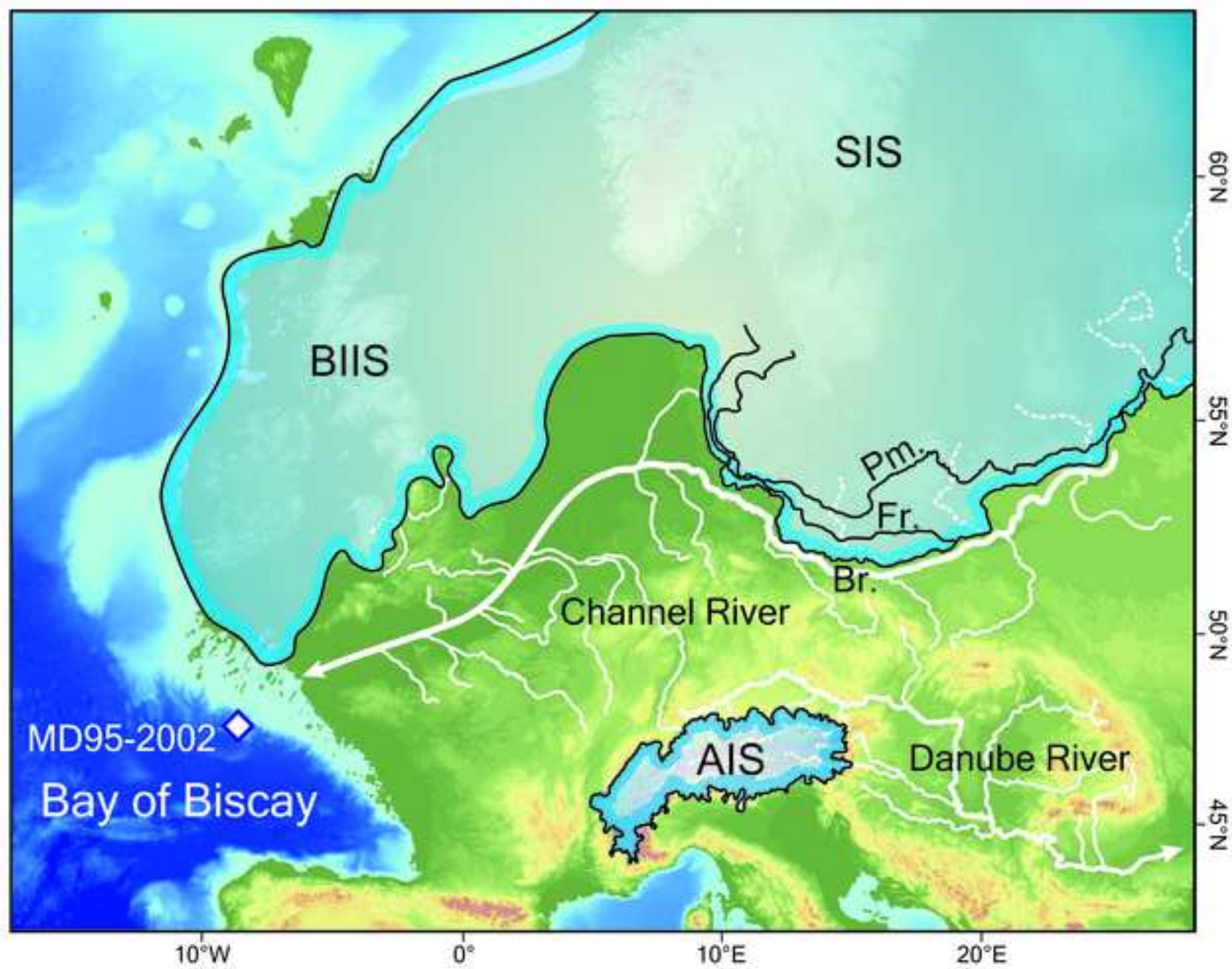
1075 Figure 5. Climate change either side of the Southern Ocean since 50 ka. Top: Southern Alps
1076 glacier-inferred temperature curve (see Figure 3). Bottom: South Pole Ice Core (SPICE) $\delta^{18}\text{O}$
1077 record (Steig et al., 2021) placed on the SP19 timescale of Winski et al. (2019). Vertical pink
1078 bars represent durations of Heinrich stadials (HS). Vertical blue bars represent episodes of
1079 Southern Alps moraine construction.

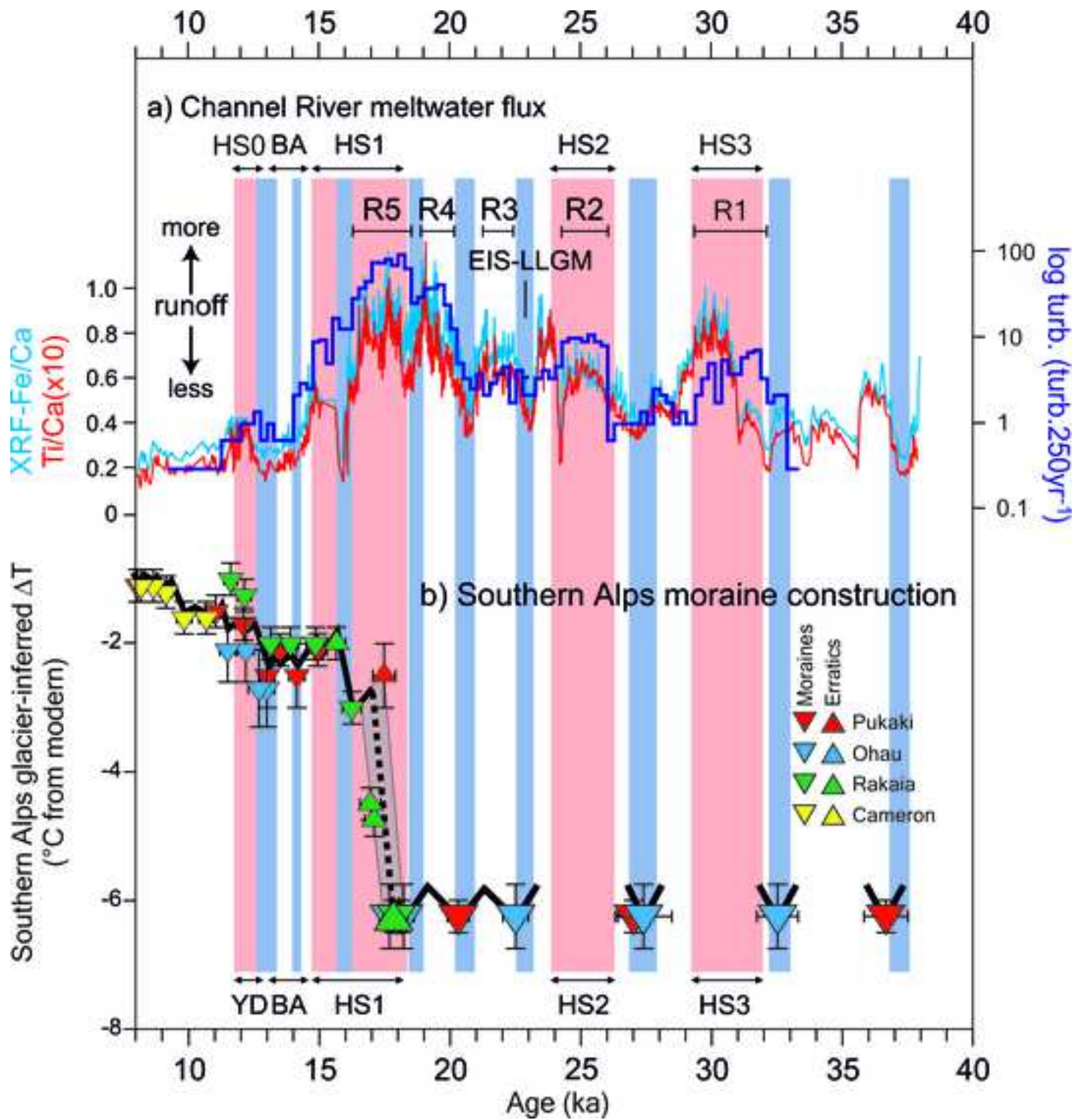
1080
1081 Figure 6. Phasing of meltwater discharges in ice-proximal settings of the North Atlantic and
1082 North Pacific during Heinrich Stadials (HS), and their relationship with Heinrich events (HE). a),
1083 NGRIP $\delta^{18}\text{O}$ (GICC05 chronology; Svensson et al., 2008) and the North Atlantic IRD stack
1084 (Stern and Lisiecki, 2013). b) Bulk carbonate as % CaCO_3 (that defines the Hudson Strait source
1085 and the HE) and $\delta^{18}\text{O}$ of the planktic polar foraminifera *Neogloboquadrina pachyderma* in core
1086 Hu97048–07, Baffin slope (Rashid et al., 2012); c) total mass accumulation rates and IRD mass
1087 accumulation rates (S_x =Siku events) at IODP Site U1419, Alaskan margin (Walczak et al.,
1088 2020); d) turbidite (i.e. flood-related deposits) flux of Baltic origin off the Channel River,
1089 (Toucanne et al., 2015); e) West Antarctic WDC $\delta^{18}\text{O}$ record (WAIS Divide Project Members,
1090 2015) with the black arrows highlighting warming episodes. The NGRIP $\delta^{18}\text{O}$ is also shown. All
1091 data sets are shown on their original published age models. The vertical red dashed lines show
1092 the timing of HE (i.e., the deposit of Hudson Strait IRD; vertical gray bars) at each site (except in
1093 c). Vertical blue bars highlight the periods of significant meltwater releases (as suggested by
1094 sediment flux and freshwater proxies) preceding HEs (vertical gray bars in b and d). Note that
1095 (1) increased meltwater flux typically continued during and after HEs; (2) if the timing of IRD
1096 deposition at each site (i.e., HEs in the North Atlantic vs Siku events in the North Pacific;
1097 Walczak et al., 2020) shows a complex pattern (i.e., lead-lag), the Cordilleran (c), European (d),
1098 and Laurentide (b) episodes of meltwater release preceding HEs are near-synchronous (within
1099 age uncertainties).

1100
1101 Figure 7. Southern Hemisphere paleoclimate records (top) compared with sea-surface
1102 temperatures (SSTs) of the North Atlantic subtropical gyre since 70 ka (bottom). Top: Southern
1103 Alps glacier-inferred temperature record (see Figure 3) superimposed upon the West Antarctica
1104 WDC temperature reconstruction (Buizert et al., 2015; Cuffey et al., 2016). Bottom: Alkenone-
1105 derived SSTs from International Ocean Discovery Program (IODP) core U1313 at 41°N in the
1106 mid-latitude North Atlantic Ocean (Naafs et al., 2013). Red arrows indicate Heinrich stadial SST
1107 warming intervals.

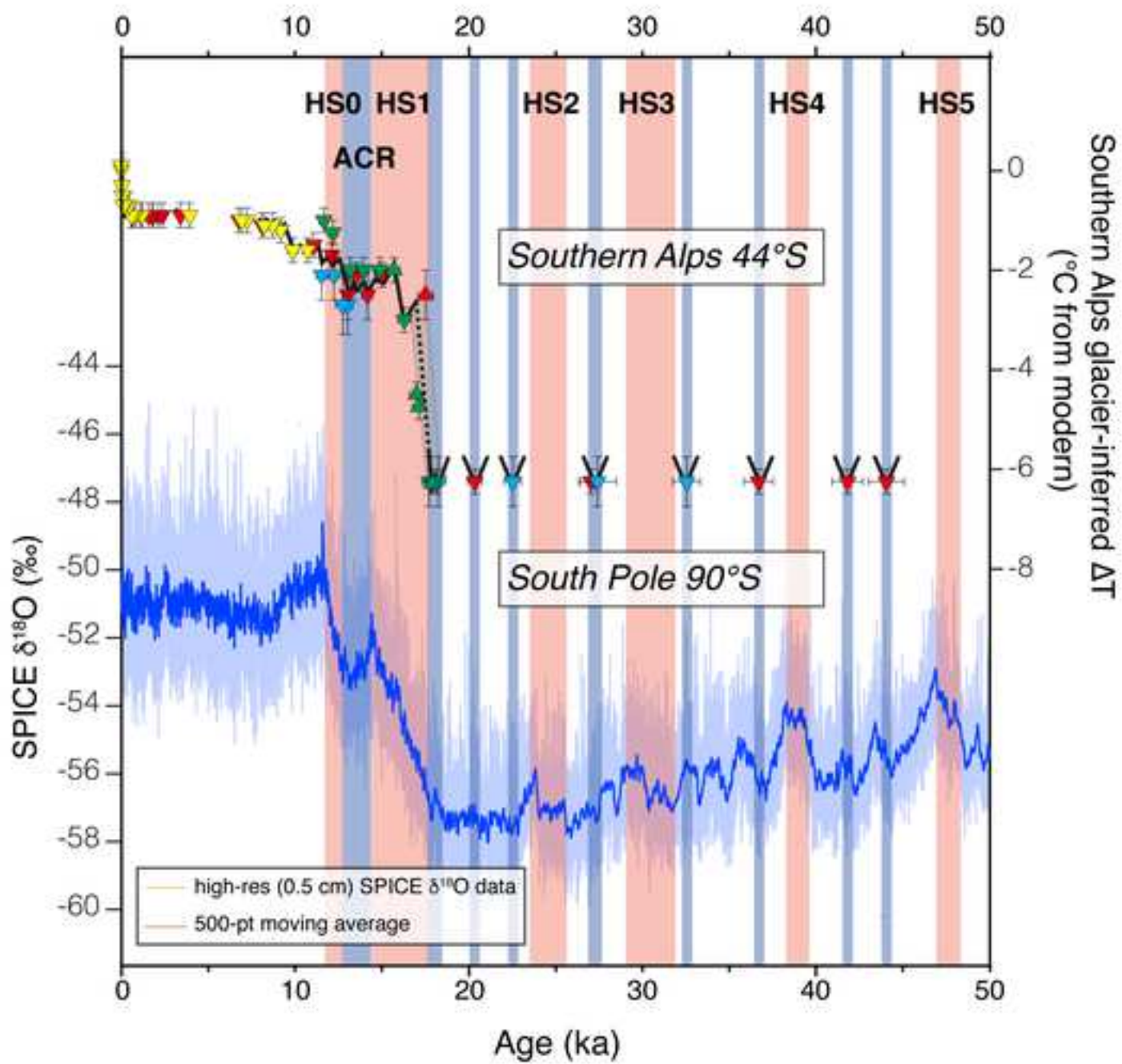
1108
1109 Figure 8. An interpretation of Younger Dryas climatic conditions in the Greenland region, used
1110 with permission and modified slightly from Broecker (2006), in turn following Denton et al.
1111 (2005). Red dots indicate the locations of the ice cores discussed in Denton et al. (2005). The
1112 mean annual temperature relative to modern is derived from the measurements of argon and
1113 nitrogen trapped in the GISP2 ice core on Summit, Greenland (Severinghaus et al., 1998). The
1114 summer temperature is from estimated snowline elevations associated with moraine belts of
1115 glaciers draining the mountains alongside Scoresby Sound (Denton et al. 2005). The winter
1116 temperature estimate represents the conditions necessary, in combination with the summer
1117 temperature estimate, to produce the mean annual temperature calculated by Severinghaus et al.,
1118 1998). Such extreme winter cold is interpreted as a consequence of the North Atlantic being
1119 extensively frozen during Younger Dryas winters.











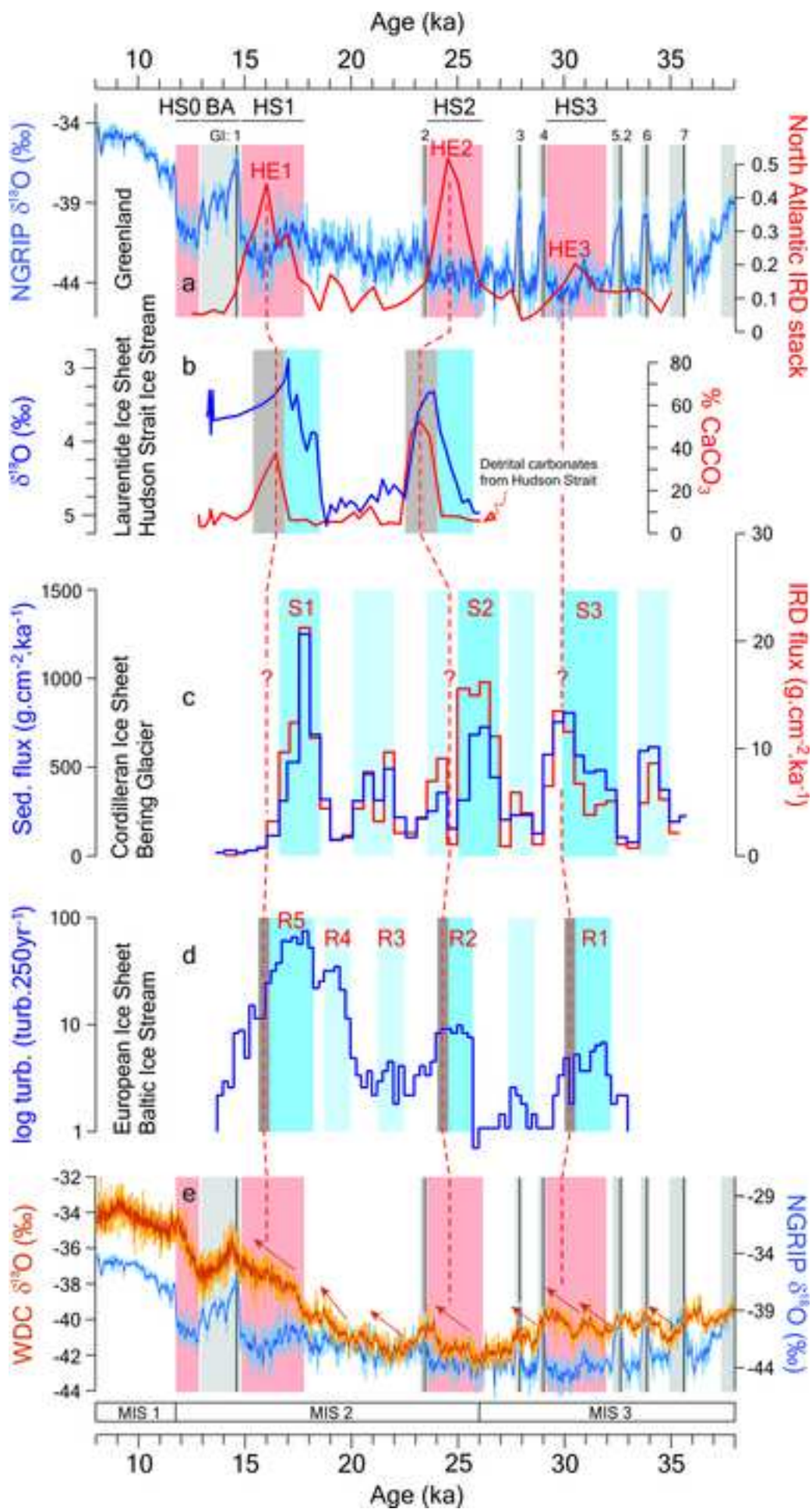
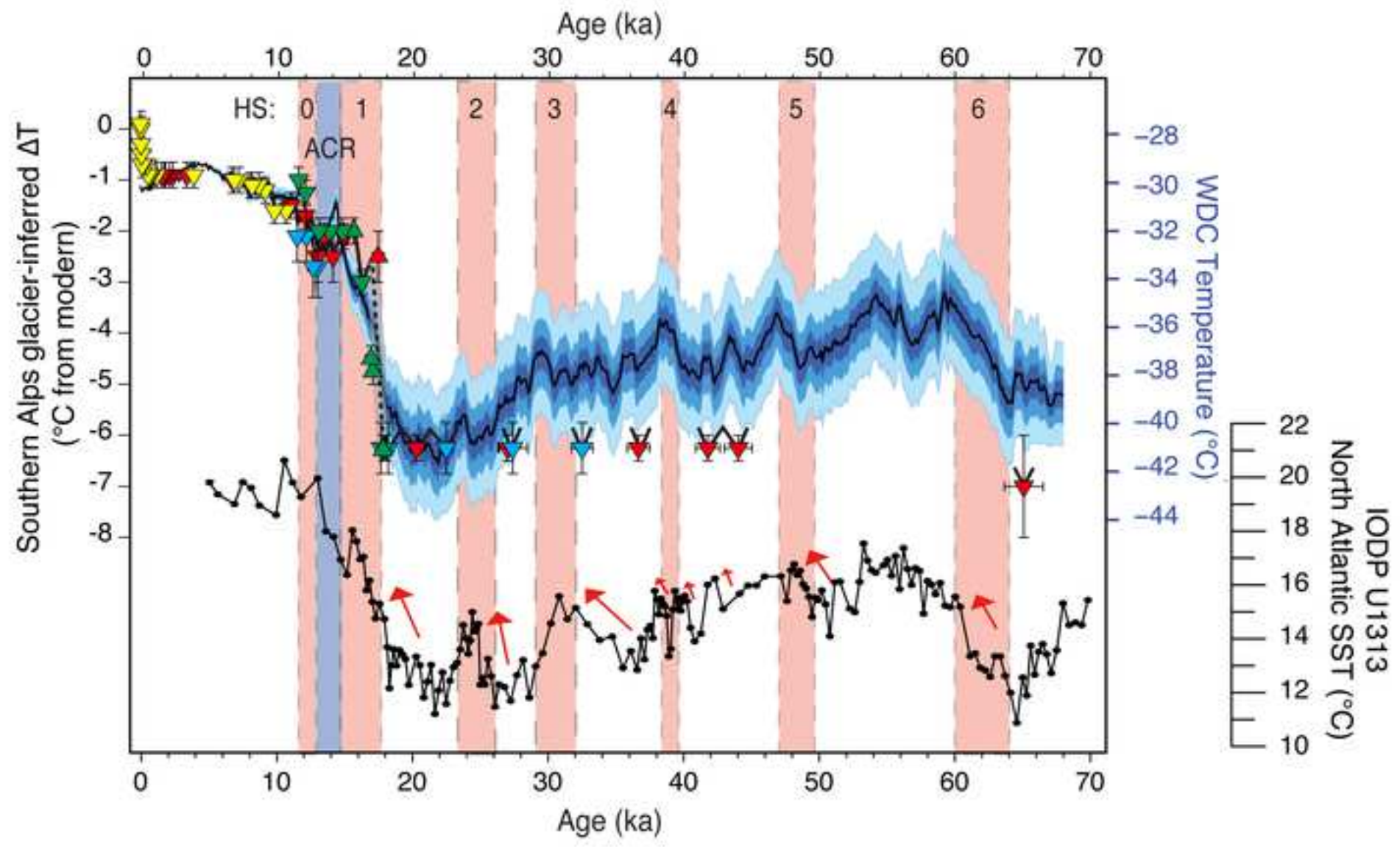
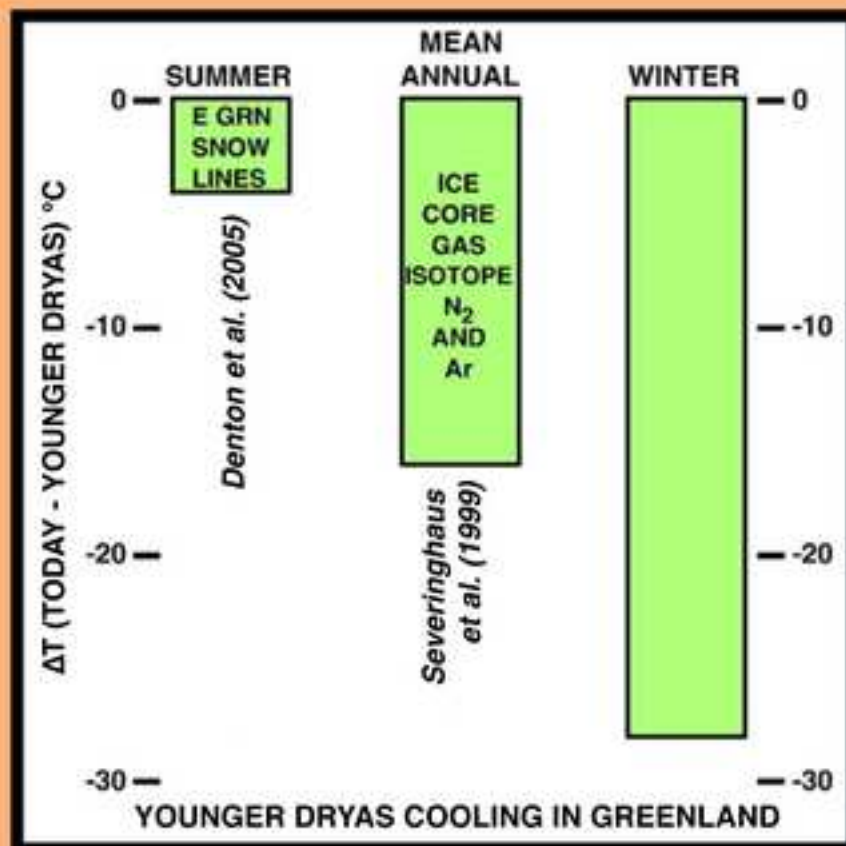
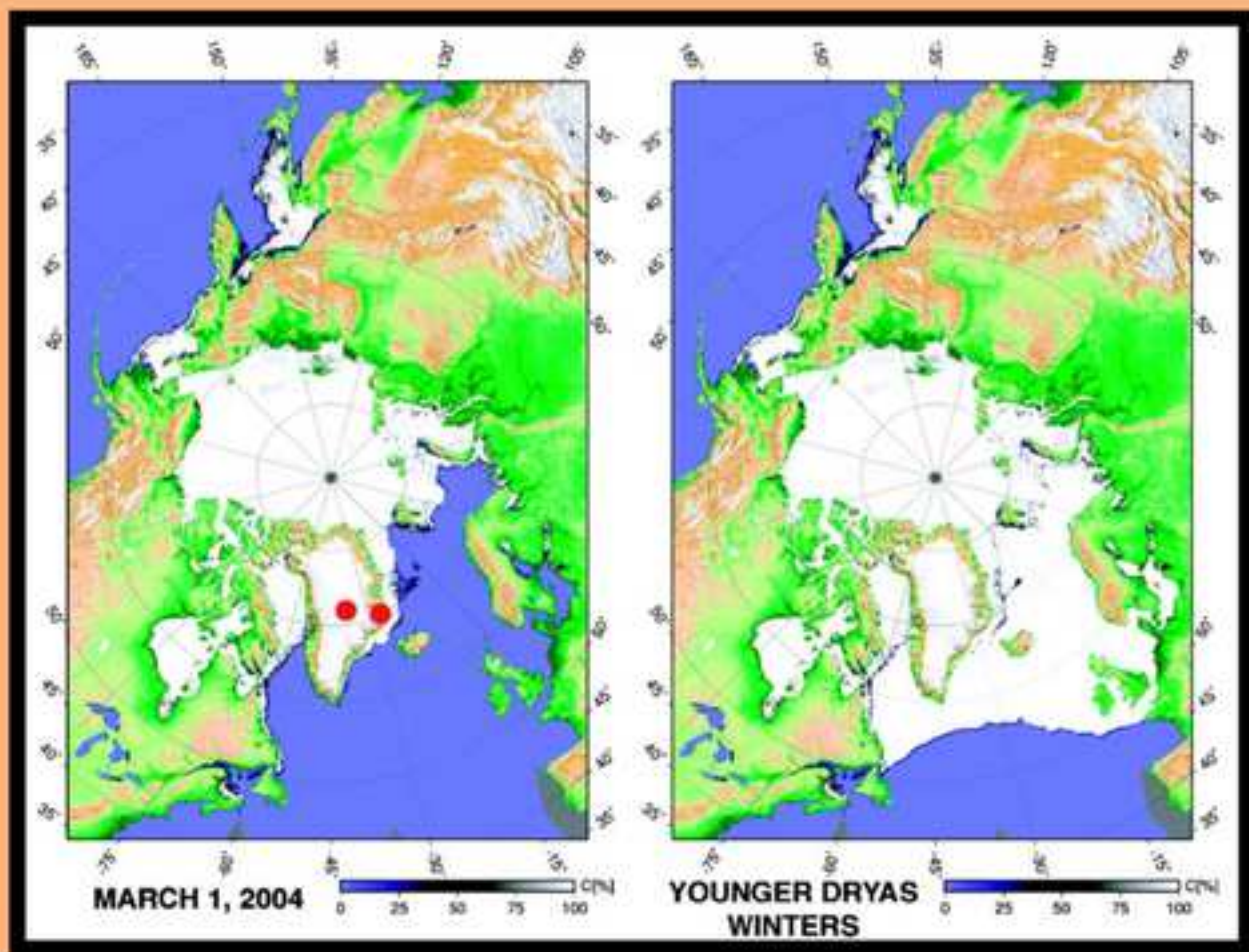


Figure 7





Declaration of interests

The authors declare that they have no known competing financial interests or personal relationships that could have appeared to influence the work reported in this paper.

The authors declare the following financial interests/personal relationships which may be considered as potential competing interests:

George Denton: Conceptualization; Methodology; Validation; Investigation; Writing – Original Draft; Writing – Review & Editing; Supervision; Project Administration; Funding Acquisition. **Aaron Putnam:** Conceptualization; Methodology; Validation; Investigation; Writing – Original Draft; Writing – Review & Editing; Visualization; Project Administration; Funding Acquisition. **Samuel Toucanne:** Conceptualization; Methodology; Validation; Investigation; Writing – Original Draft; Writing – Review & Editing; Visualization. **David Barrell:** Conceptualization; Methodology; Validation; Investigation; Writing – Original Draft; Writing – Review & Editing; Visualization. **Joellen Russell:** Conceptualization; Investigation; Writing – Original Draft; Writing – Review & Editing.